Does morphology reflect osteohistology-based ontogeny? A case study of Late Cretaceous pterosaur jaw symphyses from Hungary reveals hidden taxonomic diversity

Edina Prondvai, Emese R. Bodor, and Attila Ősi

RRH: PTEROSAUR JAW SYMPHYSIS MORPHOMETRY AND HISTOLOGY

LRH: EDINA PRONDVAI ET AL.

Abstract.—With a single complete mandible and 56 mandibular symphyseal fragments of various sizes, the Late Cretaceous Hungarian azhdarchid material has been considered one of the most extensive monospecific pterosaur assemblages in the world. Representing a broad size range, these elements have been thought to demonstrate a developmental series of *Bakonydraco galaczi*. As such, they were ideal to test whether absolute size and/or morphology reliably indicate relative ontogenetic stages in this pterosaur. Forty-five specimens were selected for multivariate morphometrics and classified into four size classes. After acquiring the morphometric data set, we thin-sectioned eight symphyses representing all size groups and classified them into relative ontogenetic stages based on qualitative microstructural inspection prior to quantitative histological analyses. Microstructural characters suggestive of developmental state were then quantified for intra- and interindividual uni- and multivariate analyses to test the correspondence among the results of qualitative and quantitative analyses. In contrast to our expectations, histological features identified the smallest specimen as an adult and not an early juvenile. The substantial size difference between this specimen and other adults, along with its distinct microanatomical and histological features, implies the presence of at least two pterosaur taxa in this symphysis assemblage. This hypothesis is further supported by multivariate morphometrics, which separate the smallest symphyses from all other specimens that form one continuous group. Although the latter group also shows considerable size variability in corresponding ontogenetic stages, this suggests developmental plasticity rather than the presence of even more taxa, and indicates that symphysis size and morphology are poor indicators of skeletal maturity in these animals. Hence, bone histology is an important independent test of the assessment of ontogenetic stage using size and morphology.

E. Prondvai and A. Ősi. Hungarian Academy of Sciences – Eötvös Loránd University "Lendület" Dinosaur Research Group, Eötvös Loránd University, Budapest, Hungary. E-mail: edina.prondvai@gmail.com

E. R. Bodor. Hungarian Geological and Geophysical Institute, Geological and Geophysical Collections, Budapest, Hungary; Eötvös Loránd University, Department of Palaeontology, Budapest, Hungary

Supplemental material deposited at Dryad:

Introduction

Pterosaur remains are usually among the rarest elements of most Mesozoic vertebrate faunas; they are predominantly isolated, fragmentary bones such as jaw fragments, teeth, vertebrae, or wing elements. Associated, articulated, and three-dimensional material is even rarer, and mostly found in fossil Lagerstätten (e.g., the Holzmaden and Solnhofen regions in Germany [Wellnhofer 1991], the Yixian Formation in the Liaoning Province of China [Wang et al. 2005], and the Araripe Basin in Brazil [Kellner and Tomida 2000; Martill 2007]) that are generally built up by finely laminated beds of shallow marine, estuarine, or lacustrine sediments. In spite of the exceptional preservation of fossils in these and sometimes other localities, only *Pteranodon*, *Pterodaustro*, *Rhamphorhynchus*, *Pterodactylus*, and perhaps *Noripterus* (Unwin and Bakhurina 2000) are represented by enough individuals to allow intraspecific statistical analysis for drawing various paleobiological inferences (Bennett 1995, 1996).

The Late Cretaceous (Santonian) vertebrate locality at Iharkút (Bakony Mountains) in western Hungary has provided numerous azhdarchid pterosaur remains, including elements from the axial and appendicular skeleton as well as from the skull. Nevertheless, the only diagnostic element known so far, on which the Hungarian medium-sized azhdarchid *Bakonydraco galaczi* was described, is a complete lower jaw (Ősi et al. 2005). Besides this uniquely preserved, three-dimensional, edentulous mandible, 56 additional symphyseal fragments have been discovered over several years of excavation, making them the most frequently found pterosaur elements in the locality. Although these additional mandibular symphyses represent a great size range, their overall appearance is practically identical to the symphysis of the holotype mandible, and therefore they have been thought to represent the largest monospecific azhdarchid pterosaur assemblage to date (Ősi et al. 2005, 2012).

In addition to their presumably monospecific origin and abundance, the completely fused mandibular symphyses are well suited for analysis because every known specimen of this skeletal element represents a single individual. With a total of 57 symphyseal fragments found so far, the Minimum Number of Individuals method (MNI), which is used in studies exploring proportional distribution of taxa in taphocenoses (Badgley 1986), gave the highest value to pterosaurs, which represent 26.6% of all vertebrate individuals at the locality (G. Botfalvai personal communication 2013). Because the sample size is sufficient for statistical analyses, this assemblage provides a unique opportunity to assess quantitatively a number of questions regarding paleobiological aspects of *B. galaczi*.

However, in order to draw sound inferences concerning ecological and even population characteristics, the initial step is to analyze the ontogenetic age composition and the proportional distribution of developmental stages of this assemblage. Although osteohistological investigation is still the most reliable method to identify relative ontogenetic stages of fossil amniotes (e.g., Horner et al. 2000, 2009; Goodwin and Horner 2004; Horner and Padian 2004; Erickson 2005; Klein and Sander 2008; Hübner 2012; Shelton et al. 2013), its destructive sampling methods often prevent the use of a statistically sufficient number of specimens of a fossil assemblage. Nevertheless, if size or other morphological characters were found to reflect the ontogenetic age of an individual, the reliable indicators would allow a reduced usage of the time- and specimen-consuming histological investigation when the aim is to study an ontogenetic series from various supraindividual perspectives.

The abundance of these mandibular symphyses made it possible for us to conduct initial tests of the degree of concordance between size, morphology, and osteohistology-based ontogenetic age, and to discuss the implications of anomalous results for further research. We investigated the relationships with different qualitative and quantitative methods, and also explored the consistency level among the independent results. Because qualitative evaluation of

bone histological characters is a conventional method for drawing various biological inferences about extinct vertebrates (e.g., Horner et al. 2000, 2009; de Ricqlès et al. 2001, 2003, 2004, 2008; Sander 2000; Chinsamy-Turan 2005; Erickson 2005; Sander et al. 2006; Klein 2010), an important element of our study is that the histomorphometric methods applied here also test how biased the qualitative judgment of measurable histological variables can be. Thus, in addition to the more species-specific points of interest, this study also presents a new methodological approach in intraspecific paleobiological research.

Materials and Methods

Material and Preparation

So far, 57 mandibular pterosaur symphyses have been collected during several seasons at the Iharkút vertebrate locality. All specimens were found while hand-quarrying the bone-yielding basal brecchia layer of the Upper Cretaceous (Santonian) Csehbánya Formation (Knauer and Siegl-Farkas 1992) in Iharkút. They were prepared in the technical laboratories of the Department of Paleontology, Eötvös Loránd University and the Hungarian Natural History Museum. Specimens were prepared with vibro-tools, needles, and localized use of 10% acetic acid. After removal of the matrix from the bones, cyanoacrylate (SuperGlue) was used to repair breaks. As is typical for most bones discovered at Iharkút (Tuba et al. 2006), the pterosaur specimens are also rich in pyrite, and the oxidation of the pyrite within them is quite rapid. The specimens were thus soaked in polyvinylacetate (PVA) or polyvinylbutyral (PVB) to stop or at least slow this process.

All specimens used in this study are housed in the Vertebrate Paleontological Collection (V PAL) of the Hungarian Natural History Museum (MTM). Hereafter we refer to these specimens only by their specimen numbers and code numbers (see below).

Reconstruction, Morphometric and Histomorphometric Measurements

Because most of these symphyses lack their anterior as well as their posterior ends, it was not possible to standardize a location for measurements and histological sampling. However, based on the holotype specimen of *B. galaczi* (2007.110.1), which represents a complete lower jaw, a relative position within the symphyseal region was assigned to each investigated specimen. For this purpose, pictures were taken of the lateral and dorsal aspects of all symphysis fragments and the holotype symphysis. An outline drawing of the holotype was made and, with reciprocal scaling, the pictures of the lateral and dorsal aspects of the specimens were placed into the best-fitting region of the line drawing of the holotype symphysis. The fit and thereby the identification of the relative positions of specimens in the symphyseal region were largely based on the angle between the dorsal surface and the ventral keel and, wherever present, on the degree of elevation and extent of the transverse ridge on the dorsal surface of the posterior end of the symphysis (Ősi et al. 2005). Because most specimens either represent the same, usually most robust, region of the symphysis, or because the relative extent of the preserved parts had considerable overlap in the symphyses, all specimens were considered suitable for further comparative analysis.

In order to explore the relationships among deduced size, morphology, and ontogeny, we classified the specimens into different size groups prior to morphometric analyses. For this, the lateral aspect of the complete symphysis was reconstructed for all specimens in the form of line drawings. Thereafter, these reconstructed symphyses were scaled proportionally, and aligned in ascending order of length (Fig. 1). Wherever a considerable increase in length was detected, a new size category was established. We arbitrarily set a 7% increase in length as the lowest limit for assigning a specimen to a larger size group. In this way, four a priori size categories (A–D) were established (Fig. 1).

Depending on general preservation state, we selected 45 of the 57 mandibular symphyses for morphometric analyses (Table 1). As for variables to measure, we selected features that were either well preserved or had states that could be inferred with high confidence in all investigated specimens, thereby circumventing the problem of missing data in the multivariate analyses. The measured variables are as follows: (1) maximum preserved width (mm), (2) maximum preserved height (mm), (3) angle between the lateral walls of the symphysis at the dorsoventrally highest point (angle of the ventral keel, α in degree), (4) angle between the lateral edges of the dorsal surface (β in degree), (5) angle between the dorsal surface and the ventral keel (γ in degree), (6) average number of foramina per 10 mm, and (7) average longitudinal diameter of foramina (mm). For an interpretative drawing of measurements see Figure 2; for values of the measured variables per specimen see Table 1.

After building the morphometric data set of the selected 45 specimens, we selected eight specimens representing all a priori defined size categories (one, two, three, and two specimens in size groups A, B, C, and D, respectively) for histomorphometric analysis (see underscored and boldface specimens in Figure 1 and Table 1, respectively). Using our reconstruction of their relative position in the symphysis, we tried to standardize the sampling location as much as possible by identifying the most probable homologous regions, i.e., finding the same relative positions along the longitudinal axis of the symphysis fragments. Cross-sections were obtained from each individual, but in five specimens longitudinal sections were also prepared in order to reveal the structural organization of the bone tissue. We selected three specimens for double cross-section sampling to explore the potential microanatomical and/or microstructural variability along the anteroposterior axis of the symphysis.

Thin-sectioning procedures followed standard methods (e.g., Wells 1989). Histological features of the acquired transverse sections were investigated under Nikon LV 100 polarized light microscope (Nikon Corp., Tokyo). Pictures of the thin sections were taken with a

QImaging MP5.0 digital microscope camera (QImaging Corp., Surrey, B.C., Canada) and processed with Image Pro Insight 8.0 (Media Cybernetics L.P., Rockville, Maryland) software. The same software was used for measuring microanatomical and histological characters.

The only microanatomical character included in the analysis was the sum of the area of extensive erosion cavities, given as the proportion (%) of total cross-sectional area. The quantified histological characters such as porosity percentage, mean vascular area and diameter, and ratio of the number of longitudinal vs. transverse vascular canals all describe vascular features in the primary cortex, thereby reflecting relative ontogenetic stages. Whereas higher values in porosity percentages and in vascular areas and diameters refer to earlier ontogenetic stages, higher ratios of longitudinal/transverse canals in the outer cortex suggest more mature developmental stages. Vascular density, expressed as the number of vascular canals per mm^2, is an unreliable measure of skeletal maturity, for if most vascular canals are organized into a network of transversely running and anastomosing canals, the actual number of individual canals, i.e., the vascular density, is lower than if the vascular architecture were characterized by much more sparse but distinct longitudinal canals. Therefore, we argue that vascular density can be successfully applied as a predictor of ontogenetic stages and/or growth rates only if the general vascular architecture of the compared regions or specimens is the same. Because it was obvious at first sight that vascular features of the dorsal, lateral, and ventral aspects of the symphysis differ considerably within a single section, we excluded vascular density from our measurements, and the retained variables were measured in each of the three symphyseal aspects separately.

We selected the best-preserved primary bone areas as measurement areas by using different polygons (mostly rectangles) following the shape of the region to measure. The measurement depth was set according to the thickness of the compacta that comprised approximately the outer fifth of the cortex and represents the last phase of development.

Ideally, the longer sides of the sampling polygon were two to three times as long as its shorter sides. On the most extensive, lateral side of the symphysis, wherever possible, two polygons were placed, one more dorsally and one more ventrally, to account for potential differences along the dorsoventral axis of the symphysis. Porosity percentage was calculated by measuring the area of all vascular canals and calculating the sum expressed as a percentage value of the total area of the polygon. Vascular spaces that were at least four times as long as wide or longer were defined as transverse canals; below that ratio all canals were identified as longitudinal canals. The 1:4 minimum width-length ratio was set based on the observation that slightly obliquely running longitudinal vascular canals have a more standard elliptic shape, with ratios always above 1:4 in transverse section. We measured the vascular diameter of the longitudinal canals as the maximum span of the circular canals and as the shorter diameter of the oval canals, whereas in transverse canals we usually measured the middle section perpendicular to the wall of the canal. In networks of transversely running channels, we measured more sections to represent both narrower and wider parts of the vascular spaces.

For comparative purposes, we derived two indices from vascular diameter and area values that standardized these values for absolute size. These indices were calculated by dividing overall mean vascular diameter and area by total area of the cross-section. To quantify measurement error, we tested area as well as diameter measurements ten times on the same 25 vascular spaces. This test showed that the mean values of area and diameter had a standard error of 1.18% and 1.65%, respectively. We therefore considered the values of the variables measured with these methods reliable for quantitative analysis.

Qualitative Histological Analysis

The qualitative description of bone histology follows the concepts and new terminology introduced by Stein and Prondvai (2013), but the basic terminology used for describing

vascular architecture is taken from Francillon-Vieillot et al. (1990). By comparing their overall, size-independent histological appearance at the same scale, we were able to assign the eight specimens to relative ontogenetic stages prior to quantitative data analysis. To do this, we investigated histological characteristics reflecting the general pattern of growth and maturation of bone tissues, and thus correlating with the ontogenetic age of the animal. These include mostly vascular features, such as vascular architecture and density, and the relative compactness of the vascular canals, the relative extent of secondary remodeling, and the relative amount of woven bone in the cortex (see e.g., Chinsamy 1994; Varricchio 1993; Erickson and Tumanova 2000; Horner et al. 2000, 2009; de Ricqlès et al. 2001, 2003, 2004, 2008; Starck and Chinsamy 2002; Chinsamy-Turan 2005; Erickson 2005; Klein and Sander 2008; Stein et al. 2010; Stein and Prondvai 2013). Because of the highly variable extent of erosion cavities and the uncertainties related to the development of the mandibular symphyses, we did not use lines of arrested growth (LAGs) as an indicator to assess ontogenetic ages.

As bone matures, the compactness of primary cavities and potentially the extent of bone remodeling are expected to increase throughout the cortex, whereas the vascular density, the amount of woven bone, and the number of transverse anastomoses decrease toward the outer cortical regions. These changes are associated with decreasing rate and eventually cessation of diametral bone growth. The relative ontogenetic stages defined here are based on these histological characteristics, and range from early juveniles to adults. Individuals that are in a fast growth phase with highly porous cortex and possibly high proportional amount of woven bone are considered early juveniles. Specimens with more mature histology and apparently less rapid bone deposition but still continuous or cyclical active growth are identified as late juveniles. Specimens showing well-marked slowing but not cessation of growth are defined as subadults. Finally, individuals showing mature histology with at most residual or no further growth are considered adults.

It must be noted that the histological changes characterizing bone maturation from early juveniles to adults represent a gradual transition without any distinct borders between these categories. However, considering the aforementioned problems related to LAG-count, these histology-based categories represent the most adequate size-independent ontogenetic classification of specimens, which is essential for our purposes.

Quantitative Analyses of Morphological and Histological Characters

All quantitative analyses were performed in R Gui (64 bit) free statistical software (R Development Core Team 2008). The significance level of statistical tests performed in this study was set to $\alpha = 0.05$ in most analyses except the normality test, where $p < 0.01$ was the level of rejecting the null hypothesis.

First, basic characteristics of the measured values such as distributions and relationships among variables were examined. The association between paired variables with binormal distribution and apparently linear relationship was tested using Pearson's product-moment correlation coefficient. The correlation between variables that do not conform to normal distribution or with an apparently nonlinear relationship was quantified by Spearman's rho. Thereafter, the morphometric data set was analyzed by multivariate exploratory methods such as principal component analysis (PCA), nonmetric multidimensional scaling (NMDS) from the library "vegan" (function "metaMDS"; Oksanen et al. 2013), agglomerative hierarchical cluster analysis (function "agnes"), and K-means cluster analysis (function "pam") from the library "cluster" (Maechler et al. 2013), and linear discriminant analysis (LDA) from the library "MASS" (Ripley et al. 2013). LDA was performed to test the strength of the a priori defined size groups as well as the most distinct groups outlined in the cluster analysis (Kovács et al. 2012). Wherever the requirement of multivariate normal distribution was met, statistical significance in the difference of multivariate group means was tested by one-way MANOVA,

after which multivariate means were contrasted pairwise by Hotelling's T-squared test with Benjamini-Hochberg correction of *p*-values. Nonparametric Wilks' λ distribution test was used to define which predictor variables played the greatest role in separating the groups. Wilks' λ quotient was calculated for each predictor variable (*x*) after Afifi et al. (2004) and Hatvani et al. (2011) as follows:

$$\lambda = [\Sigma i\, \Sigma j\, (x_{ij} - x_{i\_av})^2]\, /\, [\Sigma i\, \Sigma j\, (x_{ij} - x_{av})^2]$$

where x_{ij} is the jth element of group *i*, x_{i_av} is the mean of group *i*, and x_{av} is the mean of the predictor variable over all groups. If λ = 1 for a predictor variable, there is no intergroup variability; i.e., that particular predictor did not affect the formation of the groups (Afifi et al. 2004). If λ = 0, then that variable affected the formation of the tested groups the most (Hatvani et al. 2011). Following Hatvani et al. (2011), the statistical significance level of the importance of each variable was set to λ = 0.3.

Because Ward's minimum variance method was applied in the hierarchical cluster analysis, we used raw data in this analysis and in the corresponding LDA testing the acquired clusters. However, standardized values were calculated for PCA and for LDA used to cross-test how well the a priori defined size categories are supported. In NMDS, data were transformed by the Wisconsin standardization method. Dissimilarity was calculated using Euclidean distance with the number of dimensions set to two. The numeric output of NMDS is a stress level that measures the "badness of fit" of the monotonic regression of the ordination distances onto the dissimilarities (Kruskal and Wish 1978).

We first analyzed the histomorphometric data set intra-individually to reveal any consistent pattern of histological characters that would help select the most informative variables for interindividual comparisons. Because the regionally measured variables mostly showed right-skewed distribution and had very different sample sizes, nonparametric two-sample permutation tests were applied to compare means of vascular areas and diameters of the dorsal,

lateral and ventral regions of the symphyses. To implement these tests, we used the package "coin" (Hothorn et al. 2008) to perform one-way tests with exact and approximate (Monte Carlo, 9999 permutations) null distributions of the test statistic. Thereafter, the false discovery rate of significant p-values was controlled by the Benjamini-Hochberg procedure.

Some histological variables, such as the erosion and porosity percentages and the ratio of longitudinal vs. transverse canals, are defined by a single value for each measured area of the specimen (e.g., dorsal porosity) and/or for each specimen (e.g., overall porosity), and are henceforth referred to as single-value variables. By definition, single-value variables do not have distributions that could be statistically compared within or among individuals. Nevertheless, they are still informative in several respects, and therefore were used in interindividual comparisons along with the statistically testable variables (vascular diameters and areas). On the basis of the expected changes, namely increasing or decreasing values of these histological variables during bone maturation, a presumed developmental sequence of specimens was reconstructed for each variable. As for statistically tested variables, specimens were first contrasted by conducting a pairwise comparison of their location-specific (dorsal, lateral, ventral) vascular diameter values. Subsequently, all vascular diameter values measured in the dorsal, lateral, and ventral regions were summarized in each specimen so as to form one data set of an overall vascular diameter variable for each individual. Because the pattern of region-specific vascular areas has proven to be less consistent among individuals (see below), we used only overall vascular area to compare specimens in this respect. All interindividual univariate statistical comparisons were carried out by the same pairwise permutation tests and p-value correction procedures that were applied in intraindividual comparisons. Thus, there were nine variables in total, based on which nine developmental series, i.e., ordering of specimens according to their presumed relative ontogenetic stages, were reconstructed.

To demonstrate the consistency level in the relative position of specimens among the reconstructed ontogenetic sequences, we ranked the specimens in each of the nine quantitative variables as well as calculated the mean ranks, standard deviations, and summarized ranks for each specimen. First, we assigned ranks to each specimen in each variable according to its relative position in the sequence. This rank-ordering followed the fractional ranking rules of nonparametric statistical methods. Mean ranks of specimens were calculated as the arithmetic mean of ranks over the nine variables and then used to derive summarized ranks by rounding them to integers, sorting them in ascending order, and converting this order into rank numbers again. In this sense, summarized rank numbers can be considered a guide for an average ranking of specimens over all examined variables, whereas standard deviations of the original ranks indicate consistency in the relative position of specimens in the sequences.

Finally, new data sets were derived from the original data set for multivariate interindividual comparisons. The three newly created data tables were composed of eight observations (specimens) of four, seven, and eight variables. In the four-variable setup, the percentage of erosion cavities in the entire section and the mean values of the ratio of longitudinal vs. transverse canals, porosity percentage, and vascular diameters averaged over all measured areas constitute the four variables characterizing each specimen. In both the seven- and eight-variable data set, the mean values of porosity percentage and vascular diameters measured in each region (dorsal, lateral, ventral) of the section separately and the ratio of longitudinal vs. transverse canals gave seven variables; the percentage of erosion cavities in the entire section was included only in the eight-variable data set. After correlations among all variables were examined, the histomorphometric data sets were analyzed by the same multivariate exploratory methods as in the morphometric analyses.

The same relative ontogenetic stages as defined in the qualitative analysis were assigned to each specimen in all quantitatively constructed developmental sequences on the basis of its

relative position and relation to the neighboring specimens. This approach attempts to test the correspondence between qualitative evaluation and quantitative histoanalytical techniques by exploring whether the qualitative assessment of ontogenetic series is supported by the quantitative analyses of some of the same histological characters.

In the end, results of the quantitative multivariate morphometric and univariate and multivariate histomorphometric analyses were evaluated in the context of the a priori defined size categories and the ontogenetic classification based on the qualitative histological considerations.

Graphical Display

All figures in this study were constructed using CorelDRAW X5 (Corel Corp., Ottawa, Canada) and Photoshop 7.0 (Adobe Systems, California, USA) software. Color coding of specimens (blue, red, black, and green) denotes their a priori defined size classes (A, B, C, and D, respectively), whereas symbols (circle, square, hexagon, and diamond) assigned to the eight thin-sectioned specimens indicate their qualitatively defined ontogenetic stages (early juvenile, late juvenile, subadult, and adult, respectively).

For easier discussion and graphical representation, the correct specimen numbers have been replaced by numbers from 1 to 45, reflecting the relative position of the specimens in increasing order of the reconstructed symphysis length (see Fig. 1). Specimens are referred to as sp.1, sp.2,…, sp.45 in the text and Supplementary Material, and only by their assigned code numbers in figures and tables. For identification of correct specimen numbers by the assigned code numbers, see Figure 1 and Table 1.

Results

Reconstructed Size vs. Qualitatively Defined Developmental Stage

Comparison of the order of the eight thin-sectioned symphyses based on their reconstructed length vs. qualitatively defined (i.e., size-independent) ontogenetic sequence reveals little correspondence between absolute size and the presumed ontogenetic stage in these specimens. Whereas reconstructed symphyseal length arranges the sectioned specimens in increasing size order as sp.2 (32 mm) < sp.7 (69 mm) < sp.18 (80.5 mm) < sp.26 (95.5 mm) < sp.27 (96 mm) < sp.37 (111 mm) < sp.41 (124 mm) < sp.42 (126 mm) (Fig. 1), the qualitatively defined ontogenetic series of specimens from juveniles to adults is sp.18 < sp.27 = 41 ≤ sp.37 = sp.7 = sp.2 ≤ sp.26 = sp.42. Substituting specimen numbers with their size-group memberships, the two sequences can be listed as A < B < B < C < C < C < D < D on the basis of size, and as B < C = D ≤ C = B = A ≤ C = D according to the qualitatively assessed developmental stages. Although its minute size suggested that sp.2 represented the earliest juvenile in the developmental series of *Bakonydraco galaczi*, qualitative inspection of its histology indicated that it was a skeletally much more mature, at least subadult individual. On the other hand, the second largest sectioned specimen, sp.41, which was thought to be an adult, showed much less mature, late juvenile histological characteristics. Only the largest sectioned specimen, sp.42, showed consistent position in both sequences, whereas all other specimens occupied different relative places in the two series.

Morphometrics

The Shapiro-Wilk normality test showed that the values of all but two morphometric variables are normally distributed ($p > 0.05$). The two exceptions were α (angle of the ventral keel) and the number of foramina/10 mm—with $p = 0.001$ and $p < 0.001$, respectively—both of which have right-skewed distributions. Thus, correlations between these and other variables

were quantified by Spearman's rho. Significant positive correlations were detected between width and height ($r = 0.8$, $p < 0.001$), width and diameter of foramina ($r = 0.55$, $p < 0.001$), height and γ (angle between the dorsal surface and the ventral keel) ($r = 0.37$, $p = 0.011$), height and diameter of foramina ($r = 0.71$, $p < 0.001$), and γ and diameter of foramina ($r = 0.47$, $p < 0.001$). Significant negative correlations characterized the relationship between width and number of foramina (rho = -0.41, $p = 0.005$), height and number of foramina (rho = -0.47, $p = 0.001$), α and γ (rho = -0.45, $p = 0.002$), and number and diameter of foramina (rho = -0.35, $p = 0.018$). The remaining pairs of variables were not significantly correlated.

The strongly right-skewed distribution of α and the number of foramina/10 mm could not be normalized because removing the outliers causing this skewedness would have removed the three smallest specimens, which are of crucial importance in this study. Therefore raw or standardized values were used in our multivariate analyses, keeping in mind that LDA would have worked better on normally distributed data. The rest of the multivariate analyses used in this study do not require normal distribution.

PCA.—Based on the scree plot of principal components, PCA revealed four PCs of considerable importance in data structuring, of which PC1 accounted for the majority (50.15%) of the variance, whereas PC2, PC3, and PC4 had approximately equal eigenvalues (16.59%, 13.38%, and 10.29%, respectively). Among the measured variables, height, foramen diameter, number of foramina, and width contributed the most and almost equally to PC1; number of foramina decreased as the rest of these variables increased. The angle variables contribute predominantly to the abstraction of PC2, PC3, and PC4, with variable directions of change with respect to each other along the PC axes. For more details of the results see Supplementary Table 1.

Color-code indication (see online versions of the figures) of a priori size categories in the plot of PC1 and PC2 (Fig. 3A) clearly showed that the smallest specimens (in blue), sp.1, sp.2,

and sp.3 group farthest from the rest of the specimens, which form a more or less continuous cloud of points on PC1. No such separation is evident on PC2. The color-coding of a priori size categories in Figure 3 indicates a gradual arrangement of specimens along a size axis on PC1. No such alignment corresponding to a priori size classes can be observed on PC2. The scatter plots of PC2-PC3 and PC3-PC4 do not reflect any obvious grouping of the specimens. No spatial arrangement of specimens reflecting qualitatively defined ontogenetic categories can be observed on any of the PC scatter plots.

NMDS.—After one round, an ordination was provided with a stress level of 0.0773, which can be considered a good fit (Kruskal and Wish 1978). The ordination plot (Fig. 3B) suggests that the smallest specimens (in blue), sp.1, sp.2 and sp.3 cluster together and far from the rest of the specimens on axis 1. No other distinct groups form on this axis, but color-coded size categories seem to be arranged along a gradient. Axis 2 does not organize specimens in any obvious groups; however, to a limited degree, this axis seems to reflect the qualitative ontogenetic sequence of the thin-sectioned specimens.

Cluster Analysis.—Four major groups were delineated by the dendrogram of the hierarchical agglomerative cluster analysis (Fig. 4A). Once again, the three smallest specimens of size category A (blue) form one separate cluster (a), whereas each of the remaining three groups is composed of a mixture of a priori size categories. The next cluster most closely linked to the group of smallest specimens (d) is formed by 14 specimens, four of which belong to size class C (black), whereas the rest belong to size class B (red). The third cluster (b) consists of nine specimens in which, with the exception of sp.32 representing size class C, all specimens are categorized in size class B. The fourth cluster formed by the remaining 19 specimens includes a single specimen of size class B (sp.20), the rest of size class C, and all specimens of size class D (green). The distribution of representatives of different qualitative ontogenetic stages does not follow any regular pattern or order in this dendrogram (see assigned symbols).

K-means cluster analysis with four pre-defined groups resulted in clustering the same specimens in the same groups as in hierarchical clustering except for sp.25, which became the tenth member of the group 'b' of hierarchical clustering. Thus, grouping 44 of 45 specimens in the same way gives 97.8% correspondence between the results of the two different clustering methods.

Validating a priori Size Groups and Clusters with LDA.—Using the four a priori size categories as the grouping variable on the standardized data set in LDA, the first and second discriminant function (LD1 and LD2) account for 86.7% and 12.7% of total between-group variance, respectively. In both LD1 and LD2, number of foramina, height, and α play the most important role in the separation of the first and second groups. The number of foramina and α show negative relationship with height in LD1, whereas the interrelationship between these variables is positive in LD2. On the stacked histogram of LD1 values (Fig. 5, lower right) size group A (smallest specimens) is clearly separated from all the other size groups, because there is no overlap in their values. LD1 also separates size groups B and D, but there is considerable overlap between size groups B and C, and C and D. The histogram of LD2 values (Fig. 5, upper left) demonstrates that size group A is still distinct from B; however, values of A, C, and D, and those of B, C, and D overlap broadly. The table of correct classification and the scatter plot of LD1-LD2 (Fig. 5) show that there are 0, 1, 5, 1 specimens of a priori size groups A, B, C, and D, respectively that are misclassified by LDA. Hence, no discriminant function is able to perfectly distinguish size groups B and C, and C and D, which suggests that size group C is a transition between B and D rather than a separable, justified morphoclass. For more details of the results see Supplementary Table 2.

Because the difference in the grouping of specimens between the results of hierarchical and K-means cluster analysis was restricted to the position of one specimen, cluster validation by LDA was applied only to the results of the hierarchical analysis based on raw data. LD1 and

LD2 accounted for most of total between-group variance, 81.2% and 10.97%, respectively. In both discriminant functions, the number of foramina has the greatest and the diameter of foramina the second-greatest role in the discrimination of groups. However, the relationship between these two variables is negative in LD1, whereas it is positive in LD2. Stacked histograms (Fig. 4B) as well as the scatter plot of LD1 and LD2 indicate that the separation of cluster groups by LDA is very similar to those of a priori size groups. Cluster group 'a' on LD1 is distinct from clusters 'b', 'c', and 'd'. Cluster 'c' has no overlap with cluster 'd', but cluster 'b' and 'c', and cluster 'b' and 'd' overlap. On LD2, cluster group 'a' is separated from cluster groups 'b' and 'd', but overlaps 'c', and cluster groups 'b', 'c', and 'd' all overlap. The table of correct group identification demonstrates that there is 100% correspondence between the composition of the four groups identified by the hierarchical cluster analysis and the group memberships predicted by LDA. This suggests that cluster groups represent well-supported morphological categories. For more details of the results see Supplementary Table 3.

Testing the Significance of Predictor Variables in a priori Size Groups and Clusters with Wilks' λ.—Wilks' λ distribution test indicated that the number of foramina ($\lambda = 0.184$) and height ($\lambda = 0.256$) played a significant role in the distinction of a priori size groups. Clusters were best separated by the same variables ($\lambda = 0.203$ and 0.224, respectively) and by α ($\lambda = 0.293$).

Assessments of the Different Multivariate Methods.—The highly congruent results of the multivariate analyses applied on the morphometric data set reveal size as the most important factor in data structuring. PCA and LDA also showed how morphology alters with increasing size of the symphysis: as height and width increase, foramina on the dorsal surface become larger and more distantly spaced along the long axis of the symphysis, and the ventral keel becomes deeper (increasing γ) and more acute (decreasing α). Results of the pairwise correlation analyses of morphological variables entirely support this scenario. Wilks's λ

confirms the significance of the variables number of foramina, height, and α in the grouping of specimens in the defined multidimensional morphospace. Because angle-variables (α, β, γ) are closely associated with PC2–4, and the relative values of these variables greatly change along the length of the symphysis, PC2–4 most probably represent morphological changes along the anteroposterior axis of the symphysis. This variance most likely can be traced to the uncertainty in the exact positions on the symphysis that are occupied by largely fragmentary specimens.

Visualization of the relative position of specimens in multidimensional morphospace by scatter plots, histograms, and dendrograms of different exploratory multivariate methods showed that the most consistent pattern was the distinct separation of the three smallest symphyses (size class A) from the rest of the specimens (size classes B, C, D). However, the clear separation of the smallest size class on every plot suggests that morphological characters other than absolute size also play a role in the distinction of these three symphyses from all other specimens. This hypothesis is further supported by the observation that the three smallest specimens stay close to each other on those axes, where the spatial arrangement of the rest of specimens is obviously not directed by their size, such as on PC3 and PC4, on axis 2 of NMDS, and on both size- and cluster-validating LD3. Hence, distinction of the smallest size category (A) is verified by four independent multivariate analyses, and thereby considered a real morphoclass. On the other hand, morphology does not separate the members of size class B from C or C from D; however, size classes B and D do not overlap in multidimensional morphospace.

Qualitatively defined ontogenetic stages of the eight thin-sectioned specimens are not reflected on any of the graphical displays of the different morphometric multivariate analyses (symbols in Figs. 3–5). Thus, apart from size, no other potential structuring factor could be observed that would have produced a consistent, size-independent ordering of these specimens across the results of different morphometric multivariate methods.

Descriptive Histology

The microstructural preservation of the sectioned specimens is generally good; however, sp.2 exhibits a lot of dark staining that obscures the original histological features of its extensive cortical areas (Fig. 6D). In cross-section, the general shape of most sectioned symphyses is an isosceles triangle placed on its apex so that its base forms the dorsal surface of the symphysis (Fig. 6A,B,C). Being slightly wider than deep, the only specimen that has a shape closer to an equilateral than to an isosceles triangle is sp.2 (Fig. 6D). The overall histology of the eight selected specimens is similar with respect to bone tissue composition, spatial arrangement of primary and secondary bone tissue, and microanatomy. Regarding microanatomy, there is a system of large erosion cavities positioned mainly centrally along the sagittal axis but also invading more lateral and laterodorsal regions of the cortex (Fig. 6). The arrangement of cavities in sp.2 is slightly different from that in the other specimens, in that there is a large central cavity that does not expand in the sagittal plane but rather is restricted to the center of the cross-section, and appears much more similar to the medullary cavity of long bones (Fig. 6D). In the cross-sections of sp.18, sp.37 (Fig. 6B), and sp.41, the nutritive foramina of the dorsal surface are exposed, showing either secondarily deposited lamellae at the base of the foramen or a simple pit surrounded by primary bone tissue. No other histological feature seems to characterize these foramen pits.

The eight sectioned specimens all show a densely vascularized cortex with locally different primary vascular architecture that can be characterized in transverse section by a transitional change from the ventral to dorsal regions. Whereas dense radial to reticular vascular canals prevail through the ventral and ventrolateral compacta, the ratio of longitudinal to transverse canals increases in the dorsolateral walls, and eventually longitudinal canals dominate the dorsal part of the cortex. This gross pattern of vascular architecture is consistent in the cross-

section of each specimen. On the other hand, in longitudinal sections the channels run mainly longitudinally with random to reticular anastomoses. Both section planes reveal that vascular canals become gradually sparser toward the dorsal surface and their lumen appears much wider in the dorsal part of the symphyses than in any other cortical region. Where no erosion cavity invades the primary cortex in the central and upper-central part of the symphysis, vascular canal density is lower than in more peripheral areas. Interestingly, channels are not only present in the outermost cortex but they also open onto the periosteal surface, even in the histologically most mature specimens. Accordingly, the external fundamental system (EFS), defined as an avascular outermost cortex with densely packed growth lines and usually circumferential lamellae (Cormack 1987), could not be observed in any of the specimens. Nevertheless, closely packed but indistinct lines of arrested growth (LAGs) in the outermost cortex could be recognized in the dorsal symphyseal region of sp.37 and faintly in sp.42. By contrast, one to five relatively distantly spaced intracortical growth lines are distinct in most specimens (see e.g., Fig. 7A). The only exception is sp.2, in which no LAG could be revealed, although black staining might have obscured such structures.

The general structural organization of the periosteal primary bone tissue could be inferred from the combination of transverse and longitudinal sections (Fig. 7). Lacunocanalicular features and the optical behavior of the bony matrix under crossed plane polarizers indicate that most of the tissue is highly organized primary bone (HOPB; Stein and Prondvai 2013) with predominantly longitudinal arrangement. Accordingly, the osteocyte lacunae appear rounded and small in cross-section (Fig. 7B,C), but long and spindle shaped in longitudinal sections (Fig. 7F). The matrix of longitudinal HOPB is dark in cross-section (Fig. 7B), whereas in longitudinal section it shows strong birefringence under cross-polarized light (Fig. 7D,E,F). However, primary bone in the dorsal region has interweaving rather than longitudinal structure; the orientation of its fibers and osteocyte lacunae changes in an orderly way, and the tissue has

a braided appearance under crossed plane polarizers. Restricted patches of woven bone are sparsely distributed in the periosteal cortex of sp.18 (Fig. 8). Most of these patches consist only of two to five cell lacunae that show definite characteristics of being derived from static osteogenesis (Fig. 8) and thereby represent real woven bone (Stein and Prondvai 2013). Unambiguous woven bone could not be identified in any other specimens.

Secondary remodeling of the periosteal primary cortex is generally low and occurs mostly in areas adjacent to or within the erosion cavities (Fig. 7A–C). Whereas scattered secondary osteons are typically of the compressive type (Ascenzi and Bonucci 1967, 1968), the more extensive secondary infillings of some cavities and large remodeled areas next to the central cavities have interweaving fiber orientation and hence an unorganized appearance with variable optical behavior under cross-polarized light (Fig. 7B). Osteocyte lacunae follow this interweaving fiber orientation, and therefore are cut in diverse planes. Accordingly, the lacunae in these remodeled areas appear to have variable shapes and larger volumes compared to the uniformly transversely cut lacunae in the longitudinal HOPB in cross-sections (Fig. 7C). However, those lacunae in the secondary bone that happened to be cut longitudinally exhibit the same size and shape as the lacunae in the HOPB in longitudinal sections (compare longitudinally cut lacunae "lol" in Figure 7F). This observation illustrates Stein and Prondvai's (2013) remarks on the effect of section planes on the diverse appearance of lacunae.

Specimens sp.18, sp.27, and sp.41, which have been double cross-sectioned within a distance of less than one-eighth of their reconstructed symphysis length, showed that the erosion cavities become considerably more extensive posteriorly, and eventually they form one confluent cavity that may be called a medullary cavity. The percentage area of erosion cavities is 3.4-5.4 times higher in the more posterior than in the more anterior sections, indicating that, within one individual, compactness becomes higher toward the tip of the symphysis. In the

most posterior sections, the compacta becomes considerably thin and has only a couple of

bracing trabeculae in the medullary cavity.

Quantitative Univariate Histological Evaluation

Intraindividual Analyses.—Although statistically not testable, single-value variables, such

as region-specific porosity percentages and ratio of longitudinal vs. transverse vascular canals,

are also informative for exploring intraindividual patterns (Table 2 and Supplementary Table

4). In 64% and 80% of all specimens, the porosity of the ventral symphyseal wall was higher

than that of the lateral and dorsal walls, respectively, and 50% showed a more porous lateral

than dorsal region. Consequently, the degree of porosity changes in 64.7% of all symphyses are

as follows: dorsal < lateral < ventral. Region-specific ratios of longitudinal vs. transverse canals

revealed that 73% and 80% of the specimens have more transverse canals in their ventral cortex

than in the lateral and dorsal walls, respectively. Furthermore, in 60% of all cases, the dorsal

cortex has more longitudinal canals than the lateral regions do. In sum, 71% of all specimens

demonstrate the following ratio reflecting vascular architecture: ventral < lateral < dorsal.

The results of pairwise comparisons of vascular diameters in dorsal, lateral, and ventral

regions of the sections by means of permutation tests with $\alpha = 0.05$ significance level showed

that in 54% of all cases the mean values of the ventral and lateral vascular diameters are not

significantly different, and in 90% of all specimens the mean vascular diameter in the dorsal

wall is significantly greater than in the ventral and/or lateral walls (corrected $p < 0.05$). Thus, in

78% of all cases the following relationship between regional vascular diameters can be defined:

lateral = ventral < dorsal. Furthermore, double cross-sectioning of three specimens

demonstrated that within one specimen there was a general correspondence in the revealed

regional pattern between the posterior and anterior sections. However, pairwise comparison of

the same areas of posterior and anterior sections showed that in six of eight comparisons,

vascular diameters were smaller in the posterior than in the anterior sections, whereas in the remaining two cases, diameters were statistically indistinguishable along the anteroposterior axis of the symphysis.

Region-specific vascular areas showed a less consistent pattern. Here, 45.4% of all specimens showed significantly smaller areas in lateral than ventral walls, and 60% and 80% of them have smaller areas in ventral and lateral than in dorsal walls, respectively (corrected $p <$ 0.05). Hence, 61.7% of all cases revealed a relation between regional vascular areas as follows: lateral < ventral < dorsal. Contrasting posterior and anterior sections of the same specimen showed that in four of eight pairwise comparisons the region-specific vascular areas in posterior and anterior sections could not be statistically distinguished, whereas in the other four cases vascular areas were significantly smaller in the posterior than in the anterior sections.

Allowing for the comparatively low consistency level in the region-specific pattern of vascular areas, we selected only region-specific vascular diameters as variables for the interindividual uni- and multivariate analyses of histological characters. Table 2 and Supplementary Table 4 show a summary of relations of region-specific vascular characteristics of the sections, with more details about the individual patterns and proportions of patterns found in the 11 sections.

Interindividual Analyses.—Means and standard deviations (SD) of measured values, derived variables, and indices computed from these values are listed in Table 3. Percentage of erosion cavity area, which was shown to increase caudally in the symphysis, had the highest value in sp.41 and the lowest in sp.42. These two specimens have the largest and second-largest total cross-sectional areas, respectively. Sp.2 has by far the smallest total section area, and sp.18 has the second-smallest.

Single-value variables as well as statistically tested variables indicative of ontogenetic stages suggest a different developmental order of specimens; however, at some points there is a

high level of consistency in the sequence (Supplementary Table 5). For instance, five of nine ontogenetically informative variables indicated that sp.18 represents the earliest ontogenetic stage among specimens. In the other four cases this specimen has the second position in the reconstructed progressive developmental sequence. Standard deviation of the ranks of sp.18 is the second-lowest of all specimens, reflecting the highly consistent early juvenile status of this symphysis. Sp.41, sp.7, and sp.27 are ordered in the front half of most sequences, corresponding to rather immature stages of the developmental series. However, a standard deviation of ranks of sp.41 is comparatively high, indicating that the relative position of this specimen varies greatly across different reconstructed ontogenetic sequences. In contrast, standard deviations of sp.7 and sp.27 are moderate and approximately equal. Four variables place sp.42, the largest sectioned specimen, at the very end of the series, and one places it second-to-last, whereas all region-specific vascular diameters assign this specimen to the front half of the sequence. Thus, in five of nine cases sp.42 is defined as an adult, whereas in the rest it seems to represent a late juvenile. This inconsistent pattern is clearly quantified by its second-highest standard deviation of ranks among specimens. The highest consistency indicated by the lowest standard deviation of ranks was assigned to sp.26, which is always found in the second half of the series representing more mature developmental states. This specimen is the second-to-last in all cases defined by region-specific vascular diameters. The relative position of sp.37 seems quite variable, because it occurs equally in the first and second halves of the sequence; however, it is more often placed somewhere in the middle rather than in the front or the back of the row. The standard deviation of its ranks is moderately high, also attesting to its variable position. Nevertheless, sp.37 most probably represents an intermediate, subadult developmental state.

Extreme changes in position and thereby the highest standard deviation of ranks characterize sp.2. However, this high inconsistency is based on two extreme conditions

represented by this specimen. On one hand, although it belongs to the smallest size category, sp.2 appears as the very last (i.e., most mature) individual in the presumed ontogenetic series on the basis of all region-specific vascular diameters and on vascular area, and was ordered as the second-to-last and third-to-last according to porosity percentage and ratio of longitudinal vs. transverse vascular canals, respectively. On the other hand, sp.2 took the first, most immature place in the case of the two size-standardized indices.

Regarding the variables themselves, three pairs ordered the specimens similarly. These pairs are (1) overall ratio of longitudinal vs. transverse canals and porosity percentage, (2) size-standardized vascular diameter and size-standardized vascular area, and (3) dorsal vascular diameter and overall vascular diameter. The succession of specimens according to overall vascular area appears to be almost a combination of the sequences of the first two pairs. Sequences determined by the rest of the variables showed much less similarity to any of the other series (see Supplementary Table 5).

The summarized ranks of specimens averaged over all nine variables (Supplementary Table 5) defined the ontogenetic sequence from early juveniles to adults as follows: sp.18 < sp.41 < sp.7 = sp.27 < sp.37 < sp.2 = sp.26 = sp.42. By comparison, qualitative inspection specified the series as sp.18 < sp.41 = sp.27 $\leq$ sp.2 = sp.7 = sp.37 $\leq$ sp.26 = sp.42 (Table 4). Thus, congruent sections as well as deviations are evident between the qualitative and quantitative histological orderings of these symphyses. The consistent position of sp.18, sp.41, and sp.27 in the front and that of sp.26 and sp.42 in the back in both series strongly supports the interpretation that the specimens in the front represent early ontogenetic stages, whereas those in the back are more mature individuals. By contrast, the position of sp.2 and sp.7 in the quantitative series suggests that sp.2 was more mature and sp.7 was less mature than reconstructed in the qualitative series. Sp.37 is positioned in the middle of both sequences, indicating its intermediate state of maturity. On the other hand, replacing specimen numbers

with corresponding size classes as B < D < B = C < C < A = C = D clearly demonstrates the strong contradiction between the size-class sequence and the ontogenetic series set by quantitative histological analyses.

Quantitative Multivariate Histological Evaluation

In multivariate analyses, mean values of variables were used for each specimen. Distribution of these mean values was normal for all variables used in multivariate histological analyses (Shapiro-Wilk normality test, $p > 0.01$). Pairwise examination of correlation of variables used in the seven- and eight-variable setup indicated positive correlation between erosion percentage and vascular diameter of the lateral wall ($r = 0.71$, $p = 0.049$), between porosity of ventral and of lateral walls ($r = 0.74$, $p = 0.036$), and between porosity of lateral and of dorsal walls ($r = 0.73$, $p = 0.040$). A negative correlation was manifested between the ratio of longitudinal vs. transverse vascular canals and the porosity of the lateral wall ($r = -0.76$, $p = 0.028$). Although no correlation was detected between the ratio of longitudinal vs. transverse canals and the porosity of the ventral and dorsal walls by using a parametric correlation test (Pearson's product-moment correlation), scatter plots of these variable pairs suggested a nonlinear relationship between them. Therefore, we used the nonparametric Spearman's rank-correlation test, which showed a negative correlation between both pairs of variables (rho = -0.97, $p < 0.001$, and rho = -0.78, $p = 0.023$, respectively). Only one pair of correlating variables was found in the four-variable setup: a negative correlation between the ratio of longitudinal vs. transverse vascular canals and overall porosity ($r = -0.75$, $p = 0.032$). No other pairs of variables showed significant correlation.

PCA.—The results of PCA with four, seven, and eight variables (PCA-4, PCA-7, and PCA-8) are very similar. PC1, PC2, and PC3 account for about 50-60%, 20-25%, and 10-20% of the variance, respectively. In each case, porosity variables contribute the most to PC1, and

the ratio of longitudinal vs. transverse vascular canals always has negative relationship with the rest of the variables. In PC2, the most important variables are vascular diameters, but the ratio of longitudinal vs. transverse canals also plays a considerable role.

The scatter plots of PC1-PC2 (Fig. 9A,B,C) do not reflect any distinct group formation of specimens; their spatial distribution seems random in all three setups. There is no detectable gradient of different a priori size categories on either axis. Instead, specimens are arranged more or less corresponding to their qualitatively defined ontogenetic stages along PC1. The consistent exceptions are sp.2 and sp.7; sp.2 is always positioned in the adult range of PC1, whereas sp.7 is situated closer to late juveniles than to subadults in each case, thereby contradicting their qualitatively predicted subadult developmental stage. The arrangement of specimens in the scatter plots of PC2-PC3 reflects neither a priori size classes nor qualitative ontogenetic stages. If PC1 reflects ontogeny, specimens can be ordered from early juveniles to adults in PCA-4 as sp.18 = sp.41 < sp.7 < sp.27 < sp.37 < sp.26 < sp.2 < sp.42; in PCA-7 as sp.18 < sp.41 < sp.7 = sp.27 < sp.37 = sp.26 < sp.42 < sp.2; and in PCA-8 as sp.18 < sp.41 < sp.7 < sp.27 < sp.37 < sp.26 < sp.42 < sp.2. For more details and summary of these results see Supplementary Table 6–9.

NMDS.—After the analysis of the data with four, seven, and eight variables (NMDS-4, NMDS-7, and NMDS-8), the ordination of specimens in two dimensions had stress levels between 0 and 0.0152, implying a good match between ordinated and original distances. Specimens are evenly scattered on the ordination plots of NMDS-4 and NMDS-8 (Fig. 9D,F), whereas the ordination plot of NMDS-7 (Fig. 9E) reveals a strong association between sp.18 and sp.27, between sp.7 and sp.41, and between sp.2, sp.26, and sp.37 on both axes. Nonetheless, in each case, specimens are largely arranged according to their qualitatively defined ontogenetic stages on axis 1, whereas a priori size classes are not reflected in any way on either of these plots. Just as in PCA, the ordination of sp.7 shows deviation from the

qualitative assignments, because it remains closer to juveniles than to subadults. Also, sp.41 appears to represent an earlier ontogenetic stage than the qualitatively assessed least mature specimen, sp.18. Provided axis 1 represents progressing ontogeny, maturing developmental sequence of specimens based on the ordination plots is sp.41 < sp.7 = sp.18 < sp.27 < sp.2 = sp.26 = sp.37 < sp.42 in NMDS-4; sp.7 = sp.18 = sp.27 = sp.41 < sp.2 = 26 = 37 < 42 in NMDS-7; and sp.41 < sp.7 < sp.18 < sp.27 < sp.2 < sp.26 = sp.37 < sp.42 in NMDS-8.

Cluster Analysis.—Dendrograms of hierarchical cluster analysis with four, seven, and eight histological variables (CL-4, CL-7, and CL-8) resulted in two, three and two major clusters, respectively, with quite different groupings of the specimens (Fig. 10A,C,E). In CL-4, the pattern revealed in the dendrogram (Fig. 10A) does not correspond to the qualitative ontogenetic stages, because both major clusters are composed of a mixture of developmental categories. K-means clustering has 100% correspondence with the output dendrogram of CL-4; hence no ontogenetic grouping of specimens could be identified with this method, either. By contrast, in the dendrogram of CL-7 the first cluster is formed by specimens identified as subadults and adults, whereas the second and third clusters group specimens of earlier ontogenetic stages (Fig. 10C). Again, sp.7, which was qualitatively designated a subadult, appears in the cluster of juveniles. Thus, the clustering of CL-7 largely reflects the qualitatively defined ontogenetic stages of specimens, and the only deviation represented by the position of sp.7 is in concordance with the results of PCA and NMDS. Results of K-means cluster analysis have a correspondence level of 75% with the results of hierarchical CL-7, but in contrast to the latter, K-means clustering does not reflect ontogeny. Although CL-8 results in subgroups that seem to reflect qualitatively defined developmental stages, the separation of the juveniles by the major dichotomy decreases the correspondence between this dendrogram and the qualitatively identified ontogenetic stages (Fig. 10E). Results of K-means and hierarchical

clustering have a correspondence level of 87.5%. Finally, none of the results of these analyses reflect a priori size classes.

Validating Clusters with LDA.—Using LDA for validating cluster groups with four, seven, and eight variables (LDA-4, LDA-7, and LDA-8), LD1 separated specimens distinctly into two groups in each case based on the stacked histograms (Fig. 10B,D,F). Furthermore, the table of correct classification of specimens showed 100% agreement between group compositions predicted by LDA and the hierarchical cluster analyses. The predictor variables that played the most important role in the separation of groups in LD1 are porosity, erosion percentage, and the ratio of longitudinal vs. transverse vascular canals. However, the relationships among these variables differ in the three setups. Whereas porosity is negatively related to the other variables in LDA-4, the most important variables have positive interrelationships in LDA-7 and LDA-8.

Because there are so many variables (seven and eight) compared to the number of observations (eight) in LDA-7 and LDA-8, one-way MANOVA could be performed only for LDA-4, where it showed that 7.11% of total variance in the discriminant scores is not explained by differences in clusters ($p = 0.032$). Hotelling's T^2 test showed a significant difference between the multivariate means of the two major clusters ($p = 0.045$). For more details on the results of cluster validating LDA see Supplementary Tables 6–8.

Testing the Significance of Predictor Variables in Clusters with Wilks' λ.—In both cases in which erosion percentage was included in the analysis (CL-4 and CL-8), Wilks' λ distribution test found that only this variable had a statistically significant effect on the formation of the two major clusters ($\lambda = 0.158$). In CL-7, on the other hand, the test identified the lateral and ventral porosity percentages ($\lambda = 0.134$ and 0.199, respectively) as most important in distinguishing the two clusters. Thus, the predominant clustering role of erosion percentage, the value of which largely depends on the relative position of the section along the anteroposterior symphysis axis, obscures the ontogenetic pattern in CL-4 and CL-8. On the other hand, Wilks' λ confirms the

importance of porosity but not that of the ratio of longitudinal vs. transverse canals in the ontogenetic patterning in CL-7.

Ontogenetic Sequences based on Multivariate Analyses.—Based on the results of PCA and NMDS with four, seven, and eight variables, six ontogenetic sequences could be established for the eight thin-sectioned specimens. The summarized ontogenetic rank order of specimens averaged over the six series is sp.18 = sp.41 < sp.7 < sp.27 < sp.26 = sp.37 < sp.2 < sp.42 (Supplementary Table 9). The standard deviations of mean ranks calculated from the multivariate sequences are considerably lower than those based on the univariate sequences (Supplementary Table 5), indicating a better agreement among the results of the different multivariate methods. Comparing this sequence with the succession defined by qualitative histological observations, that is with sp.18 < sp.41 = sp.27 ≤ sp.2 = sp.7 = sp.37 ≤ sp.26 = sp.42, reveals some congruencies as well as discrepancies. In both cases, sp.18 and sp.41 are in the front, sp.37 in the middle, and sp.42 in the back of the series representing early (early/late juvenile), intermediate (late juvenile/subadult), and mature (adult) developmental stages, respectively. The relative position of the rest of the specimens is different in the two series. Sp.7 and sp.26 are placed in a less mature, and sp.2 and sp.27 in a more mature, position than predicted by the qualitative inspection. Substitution of specimen numbers with the a priori size classes to which they were assigned in the summarized ontogenetic rank order gives the following succession: B = D < B < C < C = C < A < D. This substitution shows that the defined ontogenetic order agrees with the relative position of members of size classes B and C and that of one specimen of size class D at the very end of the series. However, the first place of size class D and the position of size class A in the ontogenetic series are in sharp contrast with their positions in the reconstructed length series.

Discussion

Correspondence between Reconstructed Size and Ontogeny

The general ontogeny-size relationship in extant amniotes would suggest that the larger an organism is, the more mature histology its skeletal elements would show. Accordingly, the smallest pterosaur symphyses should represent early juveniles, and specimens of increasing size would represent late juvenile, subadult, and adult ontogenetic stages. In contrast to our expectations, we found no such congruence between reconstructed sizes and ontogenetic stages identified by either qualitative or quantitative histology. The revealed high inconsistency between the size order and ontogenetic order of specimens can be interpreted in different ways.

Potential inaccuracy of the applied methods, i.e., reconstructing the total length of the symphyses and/or assigning relative ontogenetic stage to specimens, could result in failing to find the expected positive correlation between developmental maturity and absolute size. However, estimating these inaccuracies faces several problems. On one hand, more complete symphyses would be necessary to quantify the error in our size reconstructions. On the other hand, testing how reliably the measured histological variables reflect actual ontogenetic stages in these skeletal elements of pterosaurs is not possible, because there are no living descendants of any pterosaurs from which to draw proper inferences on this relation. Nevertheless, the histological characters considered here (mostly vascular features) are generally used in paleobiological studies as the best available indicators of developmental stages in extinct vertebrates (e.g., Sander 2000; Chinsamy-Turan 2005; Sander and Klein 2005; Sander et al. 2006; Klein and Sander 2008; Horner and Goodwin 2009; Scannella and Horner 2010; Knoll et al. 2010; Padian 2013; Shelton et al. 2013), because absolute size may not be a true measure of relative ontogeny (e.g., Johnson 1977; Andrews 1982; Galton 1982; Gibson and Hamilton 1984; Brinkman 1988; Bennett 1993; Sander and Klein 2005; Woodward et al. 2011). Accordingly, the histological variables defined in this study are assumed to be strongly

associated with ontogeny, and hence to reflect developmental stages reliably enough for our purposes.

The other possible interpretation is that the detected lack of straightforward relation between size and skeletal maturity is real. In this case, our results suggest that sp.2 is far too small to represent a subadult or adult *Bakonydraco galaczi*, the holotype symphysis of which is more than three times the length of the reconstructed length of sp.2 (32 mm vs.107 mm). Because we defined size linearly, it is important to note that in most biological objects, such as bodies of complex shape, a certain amount of increase in length results in a much higher increase in volume and thereby in mass. Witton and Habib (2010) also stressed the importance of accurate length reconstructions in body mass estimation of pterosaurs by showing that pterosaur scaling coefficients predict 100% mass increase to a 30% increase in wingspan. Thus, even if the holotype of *B. galaczi* is a fully grown adult, and sp.2 was still capable of some residual growth, this size difference in length is too large for these specimens to be conspecific.

Although size in itself does not seem to be informative concerning the developmental state of the rest of the specimens either, differences in the reconstructed length of the sampled subadult and adult specimens, sp.26, sp.37, and sp.42 (96, 111, and 126 mm) are not as striking as in the case of sp.2 (32 mm). The reconstructed lengths of all 57 known symphyses (Fig. 1) reveal a considerable interruption in the size sequence for the three smallest specimens, including the thin-sectioned sp.2: there is an 81% difference in length between these three and the next (fourth) smallest symphysis. By contrast, the rest of the specimens can be placed in a presumed continuous growth series, with a gradual length increase from 58 to 129 mm. If we still assumed that all specimens represent a discontinuous growth series of a single species, *B. galaczi*, it would be difficult to explain why the size range of 32-58 mm is missing from the fossil record. Finding taphonomic reasons for this size gap would also be difficult, because

there seems to be no size-sorting effect on the vertebrate fossils found at Iharkút (Ősi et al. 2012).

If the rest of the specimens (54 symphyses) indeed form one continuous growth series of *B. galaczi*, their histologically defined relative ontogenetic stages still indicate high intraspecific variability in adult sizes: the largest sampled juvenile specimen, sp.41, is approximately 1.3 times longer than the smallest sampled adult, sp.26. Such high variation in conspecific adult sizes may be achieved by a higher degree of developmental plasticity, a phenomenon generally described as an irreversible variation in the traits of individuals resulting from variation in the environment during development (Piersma and Drent 2003). High degree of developmental plasticity in growth trajectories is frequently found in fishes, amphibians, and non-avian sauropsids (e.g. Meyer 1987; Grant and Dunham 1990; Madsen and Shine 1993; Queral-Regil and King 1998; Wikelski and Thom 2000; Schalk et al. 2002; Spencer et al. 2006), and could have enabled the adjustment of growth rate to certain environmental and/or physiological conditions in *B. galaczi* as well. Hence, the growth trajectory of this pterosaur seems to have been more flexible than that of most ornithurine birds, mammals, and some non-avian dinosaurs which are generally thought to show little interindividual variation in growth rate and adult body size (Starck and Ricklefs 1998; Starck and Chinsamy 2002; Sander and Klein 2005).

Higher degree of developmental plasticity in the growth trajectory of *B. galaczi* is also supported by the presence of intracortical LAGs in all specimens except sp.2, indicating regularly interrupted growth and thereby more plastic growth trajectory (Starck and Chinsamy 2002). Because LAGs are frequently found in the bones of other pterosaurs (de Ricqlès et al. 2000; Padian et al. 2004; Steel 2008; Chinsamy et al. 2008; Prondvai et al. 2012), and a wide range of adult sizes has also been suggested for the Late Jurassic non-pterodactyloid pterosaur *Rhamphorhynchus* (Prondvai et al. 2012), it is very likely that developmental plasticity of this kind was not rare in Pterosauria. This hypothesis needs further testing. Nevertheless, the mature

histological features of the very small sp.2 cannot be explained even if the most extreme developmental plasticity is presumed for *B. galaczi*.

In addition, the taxonomic separation of sp.2 from the rest of the specimens, which most likely represent *B. galaczi*, is justified by other qualitative microanatomical and microstructural features as well. Major differences in sp.2 compared to all other symphyses lie in the general shape of its cross-section, the overall extent and arrangement of its erosion cavity system, and the absence of deep intracortical LAGs in its compacta. If the absence of intracortical LAGs in sp.2 is genuine and not an artifact of poor preservation, it may reflect continuous rather than interrupted growth to adulthood. In this case, the growth strategy of the small sp.2 could have been more similar to that of some large-bodied azhdarchoids reported to lack LAGs and histovariability (Steel 2008), whereas the much larger *B. galaczi* probably grew more like smaller basal pterosaurs and ornithocheiroids (de Ricqlès et al. 2000; Steel 2008), with cyclical interruptions in their growth. This suggests that adult body size is not necessarily a good predictor of interrupted vs. uninterrupted growth strategies in pterosaurs.

The presence of at least two pterosaur taxa in the Santonian vertebrate fauna of Iharkút has already been suggested, based on the incomplete mandibular glenoid (MTM V 2010.98.1) of an indeterminate pterodactyloid pterosaur found in the same locality (Ősi et al. 2011). Whether sp.2 could represent the lower jaw tip of an individual of this indeterminate pterodactyloid is hard to tell. However, the mandibular glenoid of the unknown pterodactyloid has dimensions similar to that of the holotype of *B. galaczi*, which suggests that the glenoid belonged to a pterosaur of about the same size as *B. galaczi*. By contrast, pterosaurs with a morphoclass 'A' symphysis were most probably considerably smaller than any of the former pterosaurs. Unless the mandible morphology was substantially different in morphoclass 'A', and the three smallest symphyses represent the very tip of a slender lower jaw, the reconstructed size difference implies that at least three different pterosaur groups might have been present at the locality.

This hypothesis cannot be tested without finding a complete lower jaw of a pterosaur other than *B. galaczi*. For the time being, the only firm conclusion that can be drawn is that more than one pterosaur taxon inhabited this area during the Santonian.

Morphometrics, Size Classes, and Ontogenetic Stages

The different morphometric multivariate analyses applied here collectively arrange these specimens in largely the same manner, and the major predictor (as expected) is size. However, none of these analyses was able to distinguish members of size classes B and C, and C and D, which suggests that they are not valid morphological categories. On the other hand, the consistently distinct grouping of the three smallest specimens suggests that members of size class A differ from the rest of the specimens not only in their absolute size but also in overall morphology. The analyses showed this difference to lie in the relatively higher number of foramina on the dorsal surface and the dorsoventrally flatter cross-sectional shape (i.e., larger α resulting in lower relative height) of the smallest symphyses. This difference cannot be the result of allometric growth with a distinct set of morphological features of early juveniles, because sp.2 of size class A represents a histologically mature specimen. Morphometric analyses also uniformly show that symphyseal morphology, defined by features used in this study, is not a reliable indicator of histologically defined ontogenetic stages. All of these results are entirely in accordance with the conclusions drawn from the reconstructed length and the histology-based developmental state of the specimens.

Qualitative vs. Quantitative Histology

Measuring diverse histological characters and analyzing them with uni- and multivariate methods revealed statistically significant patterns that could not have been unambiguously identified by using exclusively qualitative evaluation. They also showed consistent deviations

from some of the qualitative observations. On the other hand, these methods also quantified some histological features that are already well known in the process of skeletal maturation. Thus, quantitative analyses of bone histology helped assign our specimens to those ontogenetic stages that have been supported by most of the analyses.

First, significant differences were detected in the vascular pattern of a single individual depending on the location of measurements. Most frequently, dorsal vascular canals were the widest and had the largest mean area, whereas lateral and ventral walls had equal vascular diameters, and mean area was smaller in the lateral than in the ventral region. Although these differences all seem to suggest that the dorsal part of the symphysis is the most "vascularized," the dorsal wall has the lowest mean values of porosity percentage. This apparent contradiction is easily resolved by taking vascular architecture into account. Whereas a cross-section exposes the maximum diameter of the longitudinally running canals, this is rarely the case in transverse canals, which are cut along their longitudinal axis, and the cutting plane hardly catches the maximum width of the transverse canals. Because the dorsal region mostly has the highest ratio of longitudinal canals, high values of vascular diameters are to be expected. Nevertheless, the mean vascular area should not be smaller due to the effect of the cutting plane; in fact, preliminary qualitative inspection suggested it would be larger in transverse than in longitudinal canals. This indicates that, besides the cutting plane effect, there is a genuine regional difference in the lumen size of vascular channels, where dorsal canals are wider than either lateral or ventral canals. Qualitative examination of sections also confirms the larger lumina of dorsal vascular canals. This fairly consistent spatial pattern might indicate a predetermined spatial sequence of maturation of primary osteons during symphyseal development, which could be characterized by the earlier primary infilling of ventral and lateral vascular canals. However, it can also imply the final pattern of region-specific lumen size. Because the same pattern has been revealed in the specimens deemed most mature by

qualitative histology (sp.26 and sp.42), the latter hypothesis seems more likely. On the other hand, the low porosity percentage indicates more sparsely distributed canals in the dorsal wall, which is in agreement with qualitative observations. Along with the mainly longitudinally oriented fibers in the primary bone matrix, this vascular architecture might reflect biomechanical characteristics of the symphysis of these pterosaurs. This hypothesis needs further testing.

Undoubtedly, developmental processes are reflected in the comparison of more posterior and more anterior sections of the same symphysis. Smaller vascular diameters as well as more extensive erosion cavities found in the posterior sections suggest that the formation of the most anterior part of the symphysis took place later in ontogeny. The histological differences along the anteroposterior axis of the mandibular symphyses also draw attention to the importance of standardized sampling locations (whenever possible) in comparative histological studies (Sander 2000; Klein and Sander 2008; Stein and Sander 2009; Padian et al. 2013).

When each variable is considered, the results of the quantitative interindividual univariate histology showed a lot of deviation from what we expected to find on the basis of qualitative inspection of thin sections. In fact, none of the nine quantitatively based developmental sequences were exactly the same as the qualitatively set developmental order. Inconsistencies were also common among the quantitatively defined ontogenetic series based on different variables (see Supplementary Table 5). Some of these deviations may suggest underlying patterns that are not obvious at first sight. For instance both size-standardized variables indicate that the smallest sectioned specimen, sp.2, represents the earliest ontogenetic stage in the series. This entirely contradicts the qualitative as well as all other quantitative results, which suggest that sp.2 is at least a subadult but more probably an adult specimen. This apparent contradiction indicates that vascular diameter and area may have a theoretical minimum in the pterosaur mandibular symphysis; i.e., below a certain body size, adults of small-bodied pterosaurs

possess canals of larger diameter and area relative to their body size than the adults of larger-bodied forms do.

Other differences among the sequences are more difficult to explain and probably most of them lie in the high intraspecific variability of growth dynamics and hence histological features of these pterosaurs. However, the summarized ontogenetic ranking of specimens averaged over nine quantitative histological variables was largely in agreement with their relative positions in the qualitatively defined sequence (Supplementary Table 5) with the exception of sp.2 and sp.7. Sp.7 was qualitatively identified as a subadult, whereas in the summarized quantitative succession it occupies a juvenile position. Sp.2 was identified as a subadult in the qualitative series but unambiguously determined as an adult in the summarized quantitative ontogenetic ranking, even though the latter includes two first positions of this specimen in the cases of size-standardized variables. This implies that qualitative inspection is sensitive to scaling properties of histological features: it detected the same disproportionately wide vascular canals of this specimen relative to its otherwise mature features as did the two size-standardized variables. On one hand, these results suggests that neither of the histological variables used in this study is reliable enough on its own to be used as a single appropriate predictor of relative ontogenetic stages of these pterosaur mandibular symphyses. Conversely, investigating a number of developmentally indicative variables with univariate methods and summarizing them into the most consistent pattern (see sum rank order in Supplementary Table 5) gives an estimate of relative ontogenetic stages of a set of specimens that is fairly congruent with that derived from qualitative methods.

Exploring conformity among the results of different histological multivariate analyses as objectively as possible is more difficult. Nonetheless, the arrangement of specimens resulting from all analyses but CL-4 largely reflects relative ontogenetic stages. PCA gave much more consistent ontogenetic sequences across the three different setups than did NMDS or cluster

analysis. The outcome of cluster analysis seems to be the most sensitive to the set of variables chosen for the analysis, because, due to the predominating effect of erosion percentage, the dendrogram of CL-4 and in part that of CL-8 did not show conformity with any of the results of the other analyses. Concerning the effect of variables in organizing specimens into a developmental order, all three setups of PCA and Wilks's λ of CL-7 implied that the most decisive factor is porosity. Furthermore, the loading of ratio of longitudinal vs. transverse vascular canals in PC1 always had an opposite sign to the loadings of the rest of the histological variables. This also supports the conclusion of the qualitative observations, which predicted a higher ratio of longitudinal canals in the outer cortex of more mature individuals, whereas all other defined variables show decreasing values in later ontogenetic stages. The rank order of specimens summarized over all settings of PCA and NMDS demonstrates moderate congruence with qualitative and univariate quantitative conclusions on a finer scale, i.e., on the exact specimen order (Table 4). However, it must be stressed that sequences derived from these multivariate analyses are quite arbitrary and artificially reduced by us to a one-dimensional line so that they can be more easily compared with the qualitative and univariate quantitative results. Still, on a larger scale the conformity among the results of all of our histological analyses is considerable. That is, (1) sp.18 and sp.41 clearly represent the earliest ontogenetic stages in the series; (2) sp.27 is most probably a more mature, but still actively growing late juvenile; (3) sp.37 seems to have belonged to a subadult individual; and (4) sp.26 and sp.42 are the most mature symphyses representing adult animals. On the other hand, the juvenile position of sp.7 and the adult position of sp.2 are clearly supported by all uni- and multivariate quantitative techniques and contrast with the qualitatively defined ontogenetic stages of these specimens (Table 4).

Our study clearly shows that the results of a variety of quantitative uni- and multivariate histological analyses are highly congruent and are loaded with much less subjectivity than those

of qualitative histology. Thus, analyzing histological characters with a combination of different quantitative methods has proven reliable and essential in assessing the most supported relative ontogenetic stages of these pterosaur symphyses. This draws attention to the importance of quantitative histology in other comparative histological investigations as well, especially in those that deal with such peculiar skeletal elements as these pterosaur symphyses, the developmental process and function of which we know so little.

Good Predictors, Bad Predictors

Synthesizing our results over all qualitative and quantitative investigations demonstrates that purely qualitative morphological inspection of these mandibular symphyses, which presumed a monospecific assemblage, has proven to be a highly unreliable tool for species recognition, because all methods uniformly indicate the presence of another species besides *B. galaczi*. Hence, the evidence of a second species gained so much support by the congruent results that we can confidently distinguish the three smallest specimens from *B. galaczi* and consider them as Pterodactyloidea indet. Nevertheless, reconstructed absolute lengths are reflected in all multivariate analyses, suggesting that absolute size and changes in overall morphology are strongly correlated.

Although qualitative and quantitative histology gave fairly consistent results in predicting relative ontogenetic stages, qualitative evaluation is more prone to subjectivity and might have other pitfalls as well. Such a pitfall was represented by the underestimated qualitative ontogenetic stage of sp.2 due to scaling effects. This size dependence could be filtered out with quantitative methods when the relative position of this specimen in the case of the two size-standardized variables was drastically different from the uniform conclusions of all other uni- and multivariate analyses. It is also clear that reliance on a single histological feature, which is believed to indicate developmental stage, can be very misleading. For instance, a confusing

observation is that all symphyses, even those qualitatively referred to as adults (e.g., sp.42), showed a considerable number of vascular channels opening onto the outer surface of the symphysis. This microstructural feature is typically the sign of skeletal immaturity in the case of long bones, reflecting their capability of further diametrical growth. Therefore, the relatively extensive outer cortical vascularization was a perplexing factor during the qualitative evaluation of the symphyses. However, unlike the tendinous and fleshy attachments found on limb bones, the mandibular symphyses of azhdarchid pterosaurs were most probably covered by a keratinous sheet (Ősi et al. 2011), the nutritive sustenance of which may have taken place through the symphyses, which would account for the abundantly vascularized bone surface even in skeletally mature ontogenetic stages. If the ontogenetic sequences missed the skeletally mature developmental stage, it would be difficult to explain why adults are missing from this extensive assemblage.

By and large, the cortical porosity percentage, which incorporates the effect of vascular diameter, area, architecture, and density as well, seems to be the most reliable histological character in identifying relative ontogenetic state. Thus, we recommend that this ontogenetic indicator be precisely quantified in intraspecific histological comparisons so that the most appropriate conclusions can be drawn. However, for all the extra support and finer details that the quantitative analyses of other histological variables can provide us, we recommend qualitative evaluation along with uni- and multivariate quantitative techniques whenever possible.

Finally, no well-defined, clear-cut relationship seems to exist between either absolute size and ontogenetic stage or morphology and ontogenetic stage in these symphyses, at least based on the variables used in this study. This statement remains valid even if the three smallest specimens are excluded and only the supposedly monospecific *Bakonydraco* symphyses are taken into account. Although a set of specimens may definitely resemble an ontogenetic series,

nothing can be said about the relative developmental order of specimens based only on size differences and/or groups established by morphological multivariate techniques.

The broader implication of our results is that histological investigation may be inevitable if the research questions consider developmental issues, ecology, or population dynamics of a certain species with numerous available specimens. This is especially true of extinct species with apparently diverse growth dynamics, i.e., considerable developmental plasticity (e.g., *Plateosaurus*; Sander and Klein 2005). If the presence of deep intracortical LAGs indeed reflects developmental plasticity to some extent, as suggested by Starck and Chinsamy (2002), this growth strategy may well have characterized a wide range of derived diapsids such as most sauropterygians (Klein 2010), several dinosaurs (e.g., de Ricqlès 1983; Chinsamy 1994; Erickson and Tumanova 2000; Horner et al. 2000, 2009; Horner and Padian 2004; Erickson et al. 2004, 2007, 2009; Chinsamy-Turan 2005; Erickson 2005; Scheyer et al. 2010; Woodward et al. 2011), and a number of pterosaurs (de Ricqlès et al. 2000; Padian et al. 2004; Steel 2008; Prondvai et al. 2012; current study), as also demonstrated by this study.

Conclusions

The original aim of this study was to clarify whether 57 pterosaur symphyses, all presumed to represent a developmental series of *Bakonydraco galaczi*, show any distinctive morphological features based on which relative ontogenetic stage could be assigned to the specimens without performing destructive histological sampling on each specimen. However, instead of finding good morphological predictors of ontogenetic stages of a single species, the morphological and histological analyses strongly suggest that this assemblage is not even monospecific. This draws attention to the importance of analytical assessments of the taxonomic integrity of a fossil assemblage before asking species-specific questions related to

paleoecology and population dynamics. Furthermore, the potential significance of bone histological studies in more conventional (e.g., taxonomic) paleontological considerations has been demonstrated once again.

The variables and specimens used in this study reveal no conclusive relation between size and ontogeny or between morphology and ontogeny, even if the three smallest specimens, which are not conspecific with *B. galaczi*, are disregarded. Instead, the presence of LAGs throughout the cortices, along with the large variability in body sizes of specimens representing corresponding ontogenetic stages, strongly suggests a considerable degree of developmental plasticity in the growth of *B. galaczi*. Thus, the most reliable indicators of development in these symphyses are still the histological features. Although this may hold true only for the mandibular symphyses of *B. galaczi*, it is more likely that, for the same reasons, histological investigation is necessary to infer ontogenetic stage in other skeletal elements and/or in other pterosaurs as well.

By applying more than one method to the same hypothesis we tested the correspondence and deviations between the results produced by the different methods. Thus, our study not only improves the understanding of potential biological causes behind the revealed pattern, but also represents a simultaneous exploration of how different our conclusions would be if we preferred to use either of the applied methods by itself. From this methodological perspective, we conclude that except for one setup in the cluster analysis of histological characters, all multivariate methods give congruent results within morphometrics and histology. This correspondence demonstrates the applicability and usefulness of each of these methods even in intraspecific studies. As for the conformity between qualitative and quantitative techniques, distribution of a priori size classes agreed with the results of multivariate morphometrics, indicating that changes in absolute size correlate well with changes in overall morphology. Qualitative assessments were largely supported by the quantitative results in the histological

analyses. However, the results of the less subjective quantitative methods showed consistent differences from the qualitative assessments. Furthermore, quantitative histological analyses revealed finer details of bone microstructure that remained unnoticed by qualitative inspection.

Acknowledgments

Literature Cited

Afifi, A., V. A. Clark, S. May, and B. Raton. 2004. Computer-aided multivariate analysis, 4th ed. Chapman and Hall/CRC Press, Boca Raton, Fla.

Andrews, R. M. 1982. Patterns of growth in reptiles. Pp. 273–320 *in* C. Gans and F. H. Pough, eds. Biology of the Reptilia. Academic Press, London.

Ascenzi, A., and E. Bonucci. 1967. The tensile properties of single osteons. Anatomical Record 158:375–386.

———. 1968. The compressive properties of single osteons. Anatomical Record 161:377–392.

Badgley, C. 1986. Counting individuals in mammalian fossil assemblages from fluvial environments. Palaios 1:328–338.

Bennett, S. C. 1993. The ontogeny of *Pteranodon* and other pterosaurs. Paleobiology 19:92–106.

———. 1995. A statistical study of *Rhamphorhynchus* from the southern limestone of Germany: year classes of a single large species. Journal of Vertebrate Paleontology 69:569–580.

———. 1996. Year-classes of pterosaurs from the Solnhofen Limestone of Germany: taxonomic and systematic implications. Journal of Vertebrate Paleontology 16:432–444.

Brinkman, D. 1988. Size-independent criteria for estimating relative age in *Ophiacodon* and *Dimetrodon* (Reptilia, Pelycosauria) from the Admiral and lower Belle Plains formations of west-central Texas. Journal of Vertebrate Paleontology 8:172–180.

Chinsamy, A. 1994. Dinosaur bone histology: implications and inferences. Pp. 213–227 *in* G. D. Rosenberg and D. L. Wolberg, eds. DinoFest. Paleontological Society Special Publication 7:213–227.

Chinsamy-Turan, A. 2005. The microstructure of dinosaur bone: deciphering biology with fine-scale techniques. Johns Hopkins University Press, Baltimore.

Chinsamy, A., L. Codurniu, and L. Chiappe. 2008. Developmental growth patterns of the filter-feeder pterosaur, *Pterodaustro guiñazui*. Biology Letters 4:282–285.

———. 2009. Palaeobiological implications of the bone histology of *Pterodaustro guinazui*. Anatomical Record 292:1462–1477.

Cormack, D. H. 1987. Ham's histology. Lippincott William and Wilkins, New York.

de Ricqlès, A. 1983. Cyclical growth in the long limb bones of a sauropod dinosaur. Acta Palaeontologica Polonica 28:225–232.

de Ricqlès, A., K. Padian, J. R. Horner, and H. Francillon-Viellot. 2000. Paleohistology of the bones of pterosaurs (Reptilia: Archosauria): anatomy, ontogeny and biochemical implications. Zoological Journal of the Linnean Society 129:349–385.

de Ricqlès, A., O. Mateus, M. T. Antunes, and P. Taquet. 2001. Histomorphogenesis of embryos of Upper Jurassic theropods from Lourinhã (Portugal). Comptes Rendus de l'Académie des Sciences, série IIA 332:647-656.

de Ricqlès, A., K. Padian, J. R. Horner, E.-T. Lamm, and N. Myhrvold. 2003. Osteohistology of *Confuciusornis sanctus* (Theropoda: Aves). Journal of Vertebrate Paleontology 23:373–386.

de Ricqlès, A., J. Castanet, and H. Francillon-Vieillot. 2004. The 'message' of bone tissue in paleoherpetology. Italian Journal of Zoology 71(Suppl. 1):3–12.

de Ricqlès, A., K. Padian, F. Knoll, and J. R. Horner. 2008. On the origin of high growth rates in archosaurs and their ancient relatives: complementary histological studies on Triassic archosauriforms and the problem of a "phylogenetic signal" in bone histology. Annales de Paléontologie 94:57–76.

Erickson, G. M. 2005. Assessing dinosaur growth patterns: a microscopic revolution. Trends in Ecology and Evolution 20:677–684.

Erickson, G. M., and T. A. Tumanova. 2000. Growth curve of *Psittacosaurus mongoliensis* Osborn (Ceratopsia: Psittacosauridae) inferred from long bone histology. Zoological Journal of the Linnean Society 130:551–566.

Erickson, G. M., P. J. Makovicky, P. J. Currie, M. A. Norell, S. A. Yerby, and C. A. Brochu. 2004. Gigantism and comparative life-history parameters of tyrannosaurid dinosaurs. Nature 430:772–775.

Erickson, G. M., K. Curry Rogers, D. J. Varricchio, M. A. Norell, and X. Xu. 2007. Growth patterns in brooding dinosaurs reveal the timing of sexual maturity in non-avian dinosaurs and genesis of the avian condition. Biology Letters 3:558–561.

Erickson, G. M., O. Rauhut, Z. Zhonghe, A. H. Turner, B. D. Inouye, D. Hu, and M. A. Norell. 2009. Was dinosaurian physiology inherited by birds? Reconciling slow growth in *Archaeopteryx*. PLoS ONE 4(10):e7390, 1–9.

Francillon-Vieillot, H., V. de Buffrénil, J. Castanet, J. Geraudie, F. J. Meunier, J. Y. Sire, L. Zylberberg, and A. de Ricqlès. 1990. Microstructure and mineralization of vertebrate skeletal tissues. Pp. 471–548 *in* J. E. Carter, ed. Skeletal biomineralization: patterns, processes and evolutionary trends. Van Nostrand Reinhold, New York.

Galton, P. M. 1982. Juveniles of the stegosaurian dinosaur *Kentrosaurus* from the Upper Jurassic of Tanzania, East Africa. Journal of Vertebrate Paleontology 2:47–62.

Gibson, C. W. D., and J. Hamilton. 1984. Population processes in a large herbivorous reptile: the giant tortoise of Aldabra atoll. Oecologia 61:230–240.

Goodwin, M. B., and J. R. Horner. 2004. Cranial histology of pachycephalosaurs (Ornithischia: Marginocephalia) reveals transitory structures inconsistent with head-butting behavior. Paleobiology 30:253–267.

Grant, B. W., and A. E. Dunham. 1990. Elevational covariation in environmental constraints and life histories of the desert lizard *Sceloporus merriami*. Ecology 71:1765–1776.

Hatvani, I. G., J. Kovács, I. Székely, P. Kovácsné Jakusch, and J. Korponai. 2011. Analysis of long term water quality changes in the Kis-Balaton Water Protection System with time series, cluster analysis and Wilks' lambda distribution. Ecological Engineering 37:629–635.

Horner, J. R., and M. B. Goodwin. 2009. Extreme cranial ontogeny in the Upper Cretaceous dinosaur *Pachycephalosaurus*. PLoS ONE 4(10): e7626, 1–11.

Horner, J. R., and K. Padian. 2004. Age and growth dynamics of *Tyrannosaurus rex*. Proceedings of the Royal Society of London B 27:1875–1880.

Horner, J. R., A. J. de Ricqlès, and K. Padian. 2000. The bone histology of the hadrosaurid dinosaur *Maiasaura peeblesorum*: growth dynamics and physiology based on an ontogenetic series of skeletal elements. Journal of Vertebrate Paleontology 20:109–123.

Horner, J. R., A. J. de Ricqlès, K. Padian, and R. D. Scheetz. 2009. Comparative long bone histology and growth of the "hypsilophodontid" dinosaurs *Orodromeus makelai*, *Dryosaurus altus*, and *Tenontosaurus tillettii* (Ornithischia: Euornithopoda). Journal of Vertebrate Paleontology 29:734–747.

Hothorn, T., K. Hornik, M. A. van de Wiel, and A. Zeileis. 2008. Implementing a class of permutation tests: the coin package. Journal of Statistical Software 28:1-23.

Hübner, T. R. 2012. Bone histology in *Dysalotosaurus lettowvorbecki* (Ornithischia, Iguanodontia)—variation, growth, and implications. PLoS ONE 7(1):e29958, 1–29.

Johnson, R. 1977. Size independent criteria for estimating relative age and relationships among growth parameters in a group of fossil reptiles (Reptilia: Ichthyosauria). Canadian Journal of Earth Sciences 14:1916–1924.

Kellner, A.W. A. and Y. Tomida. 2000. Description of a new species of Anhangueridae (Pterodactyloidea) with comments on the pterosaur fauna from the Santana Formation

(Aptian–Albian), northeastern Brazil. National Science Museum Monographs 17. National Science Museum, Tokyo.

Klein, N. 2010. Long bone histology of Sauropterygia from the Lower Muschelkalk of the Germanic Basin provides unexpected implications for phylogeny. PLoS ONE 5(7): e11613, 1–25.

Klein, N., and P. M. Sander. 2008. Ontogenetic stages in the long bone histology of sauropod dinosaurs. Paleobiology 34:247–263.

Knauer, J., and Á. Siegl-Farkas. 1992. Palynostratigraphic position of the Senonian beds overlying the Upper Cretaceous bauxite formations of the Bakony Mts [In Hungarian.] A bakonyi felső-kréta bauxitformációk szenon fedőképződményeinek palynosztratigráfiai helyzete. Annual Report of the Hungarian Geological Institute 1990:463–471.

Knoll, F., K. Padian, and A. de Ricqlès. 2010. Ontogenetic change and adult body size of the early ornithischian dinosaur *Lesothosaurus diagnosticus*: implications for basal ornithischian taxonomy. Gondwana Research 17:171–179.

Kovács, J., P. Tanos, J. Korponai, I. Kovácsné Székely, K. Gondár, K. Gondár-Sőregi, I. G. Hatvani. 2012. Analysis of water quality data for scientists. Pp. 65-94 *in* K. Voudouris and D. Voutsa, eds. Water quality monitoring and assessment Rijeka. InTech Open Access Publisher.

Kruskal, J. B., and M. Wish. 1978. Multidimensional scaling. Sage University Paper Series on Quantitative Applications in the Social Sciences No. 07-011. Sage Publications, Newbury Park, Calif.

Madsen, T., and R. Shine. 1993. Phenotypic plasticity in body sizes and sexual dimorphism in European grass snakes. Evolution 47:321–325.

Maechler, M., P. Rousseeuw, A. Struyf, M. Hubert, and K. Hornik. 2013. cluster: cluster analysis basics and extensions. R package, version 1.14.4.

Martill, D. M. 2007. The age of the Cretaceous Santana Formation fossil Konservat Lagerstätte of north-east Brazil: a historical review and an appraisal of the biochronostratigraphic utility of its palaeobiota. Cretaceous Research 28:895–920.

Meyer, A. 1987. Phenotypic plasticity and heterochrony in *Cichlasoma managuense* (Pisces, Cichlidae) and their implications for speciation in cichlid fishes. Evolution 41:1357–1369.

Oksanen, J., F. G. Blanchet, R. Kindt, P. Legendre, P. R. Minchin, R. B. O'Hara, G. L. Simpson, P. Solymos, M. H. H. Stevens, and H. Wagner. 2008. The 'vegan' package. http://cran.r-project.org, http://vegan.r-forge.r-project.org/.

Ősi, A., D. B. Weishampel, and C. M. Jianu. 2005. First evidence of azhdarchid pterosaurs from the Late Cretaceous of Hungary. Acta Palaeontologica Polonica 50:777–787.

Ősi, A., E. Buffetaut, and E. Prondvai. 2011. New pterosaurian remains from the Late Cretaceous (Santonian) of Hungary (Iharkút, Csehbánya Formation). Cretaceous Research 32:456–463.

Ősi, A., M. Rabi, L. Makádi, Z. Szentesi, G. Botfalvai, P. Gulyás. 2012. The Late Cretaceous continental vertebrate fauna from Iharkút (Western Hungary): a review. Pp. 533–569 *in* P. Godefroit, ed. Bernissart dinosaurs and Early Cretaceous terrestrial ecosystems. Indiana University Press, Bloomington.

Padian, K. 2013. Why study the bone microstructure of fossil tetrapods? Pp. 1–11 *in* K. Padian and E.-T. Lamm eds. Bone histology of fossil tetrapods: advancing methods, analysis, and interpretation. University of California Press, Los Angeles.

Padian, K., J. R. Horner, and A. de Ricqlès. 2004. Growth in small dinosaurs and pterosaurs: the evolution of archosaurian growth strategies. Journal of Vertebrate Paleontology 24:555–571.

Padian, K., E-T. Lamm, and S. Werning 2013. Selection of specimens. Pp. 35–54 *in* K. Padian and E.-T. Lamm, eds. Bone histology of fossil tetrapods: advancing methods, analysis, and interpretation. University of California Press, Los Angeles.

Piersma, T., and J. Drent. 2003. Phenotypic flexibility and the evolution of organismal design. Trends in Ecology and Evolution 18:228–233.

Prondvai, E., K. Stein, A. Ősi, and P. M. Sander. 2012. Life history of *Rhamphorhynchus* inferred from bone histology and the diversity of pterosaurian growth strategies. PLoS ONE 7(2):e31392, 1–18.

Queral-Regil, A., and R. B. King. 1998. Evidence for phenotypic plasticity in snake body size and relative head dimensions in response to amount and size of prey. Copeia 1998:423–429.

R Development Core Team. 2008. R: a language and environment for statistical computing. R Foundation for Statistical Computing, Vienna. ISBN 3-900051-07-0, http://www.R-project.org.

Ripley, B., B. Venables, K. Hornik, A. Gebhardt, and D. Firth. 2013. Package 'MASS'. http://www.stats.ox.ac.uk/pub/MASS4/.

Sander, P. M. 2000. Long bone histology of the Tendaguru sauropods: implications for growth and biology. Paleobiology 26:466–488.

Sander, P. M., and N. Klein. 2005. Developmental plasticity in the life history of a prosauropod dinosaur. Science 310:1800–1802.

Sander, P. M., O. Mateus, T. Laven, and N. Knötschke. 2006. Bone histology indicates insular dwarfism in a new Late Jurassic sauropod dinosaur. Nature 441:739–741.

Scannella, J. B., and J. R. Horner. 2010. *Torosaurus* Marsh, 1891, is *Triceratops* Marsh, 1889 (Ceratopsidae: Chasmosaurinae): synonymy through ontogeny. Journal of Vertebrate Paleontology 30:1157–1168.

Schalk, G., M. R. Forbes, P. J. Weatherhead, and W. L. Montgomery. 2002. Developmental plasticity and growth rates of green frog (*Rana clamitans*) embryos and tadpoles in relation to a leech (*Macrobdella decora*) predator. Copeia 2002:445–449.

Scheyer, T. M., N. Klein, and P. M. Sander. 2010. Developmental palaeontology of Reptilia as revealed by histological studies. Seminars in Cell and Developmental Biology 21:462–470.

Shelton, C. D., P. M. Sander, K. H. W. Stein, and H. Winkelhorst. 2013. Long bone histology indicates sympatric species of *Dimetrodon* (Lower Permian, Sphenacodontidae). Earth and Environmental Science Transactions of the Royal Society of Edinburgh 103: 217–236.

Spencer, R. J., F. J. Janzen, and M. B. Thompson. 2006. Counterintuitive density-dependent growth in a long-lived vertebrate after removal of nest predators. Ecology 87:3109–3118.

Starck, M. J., and A. Chinsamy. 2002. Bone microstructure and developmental plasticity in birds and other dinosaurs. Journal of Morphology 254:232–246.

Starck, M. J., and R. M. Ricklefs. 1998. Avian growth and development: evolution within the altricial-precocial spectrum. Oxford University Press, Oxford.

Steel, L. 2008. The palaeohistology of pterosaur bone: an overview. *In* D. W. E. Hone and E. Buffetaut, eds. Flugsaurier: Pterosaur papers in honour of Peter Wellnhofer. Zitteliana B 28:109–125.

Stein, K., and E. Prondvai. 2013. Rethinking the nature of fibrolamellar bone: an integrative biological revision of sauropod plexiform bone formation. Biological Reviews 89:24–37.

Stein K., and M. Sander. 2009. Histological core drilling: a less destructive method for studying bone histology. Pp. 68–80 *in* M. A. Brown, J. F. Kane, and W. G. Parker, eds. Methods in fossil preparation. Proceedings of the first annual fossil preparation and collections symposium. Petrified Forest National Park, Holbrook, Ariz.

Stein, K., Z. Csiki, K. Curry Rogers, D. B. Weishampel, R. Redelstorff, J. L. Carballido, and P. M. Sander. 2010. Small body size and extreme cortical bone remodeling indicate phyletic

dwarfism in *Magyarosaurus dacus* (Sauropoda: Titanosauria). Proceedings of the National Academy of Sciences USA 107:9258-9263.

Tuba, Gy., P. Kiss, M. Pósfai, and A. Mindszenty. 2006. Investigation of diagenetic processes on the bone material of the Late Cretaceous dinosaur site in the Bakony Mts. [In Hungarian.] Diagenezis-történeti vizsgálatok a bakonyi felső-kréta dinoszaurusz lelőhely csontanyagán. Földtani Közlöny 136:1-24.

Unwin, D. M. and N. N. Bakhurina. 2000. Pterosaurs from Russia, Middle Asia and Mongolia. Pp. 420-433 *in* M. J. Benton, M. A. Shishkin, D. M. Unwin, and E. N. Kurochkin, eds. The age of dinosaurs in Russia and Mongolia. Cambridge University Press, Cambridge.

Varricchio, D. J. 1993. Bone microstructure of the Upper Cretaceous theropod dinosaur *Troodon formosus*. Journal of Vertebrate Paleontology 13:99–104.

Wang, X., A. W. A. Kellner, Z. Zhou, and D. A. Campos. 2005. Pterosaur diversity and faunal turnover in Cretaceous terrestrial ecosystems in China. Nature 437:875–879.

Wellnhofer, P. 1991. The illustrated encyclopedia of pterosaurs. Salamander Books, London.

Wells, N. A. 1989. Making thin sections. Pp. 120–129 *in* R. M. Feldmann, R. E. Chapman, and J. T. Hannibal, eds. Paleotechniques. University of Tennessee, Knoxville.

Wikelski, M., and C. Thom. 2000. Marine iguanas shrink to survive El Niño. Nature 403:37.

Witton, M. P., and M. B. Habib. 2010. On the size and flight diversity of giant pterosaurs, the use of birds as pterosaur analogues and comments on pterosaur flightlessness. PLoS ONE 5(11):e13982, 1–18.

Woodward, H. N., J. R. Horner, and J. O. Farlow. 2011. Osteohistological evidence for determinate growth in the American Alligator. Journal of Herpetology 45:339–342.

Woodward, H. N., T. H. Rich, A. Chinsamy, and P. Vickers-Rich. 2011. Growth dynamics of Australia's polar dinosaurs. PLoS ONE 6(8):e23339, 1–5.

Figure captions

FIGURE 1. Reconstructed lengths of 57 symphysis fragments in increasing order of size with the indication of suggested a priori size classes (A–D), and the code numbers replacing the actual specimen numbers in this study. Note that the length difference between the last and first members of size classes A and B, respectively, is 81%, whereas between those of size classes B and C, and C and D, this difference is only 7%. Specimens with underscored ID numbers are histologically sampled, while specimens drawn with dashed outline were not included in any of the quantitative analyses.

FIGURE 2. Morphometric measurements and variables defined for morphometric multivariate analyses on the example of sp.8. Abbreviations: f, foramina; fd, foramen diameter; h, maximum preserved height; w, maximum preserved width.

FIGURE 3. Bivariate plots of first two axes obtained from PCA and NMDS performed on morphometric variables. A, Scatter plot of the first and second principal components, PC1-PC2 identified by PCA. B, Two-dimensional ordination plot obtained by NMDS. Color coding (see online version) refers to the a priori size categories with blue, red, black, and green representing size classes A, B, C, and D, respectively. Symbols indicate qualitatively defined ontogenetic stages of histologically sampled specimens in which circle, square, hexagon, and diamond stand for early juvenile, late juvenile, subadult, and adult relative developmental states, respectively. Size-determined arrangement of specimens along both PC1 and axis 1 is evident and reflects increasing symphysis length from right to left. No such order corresponding to the qualitative ontogenetic sequence can be identified.

FIGURE 4. Dendrogram of hierarchical cluster analysis based on morphological characters (A), and stacked histograms of LDA (B) testing the strength of the four major clusters (a, b, c, d) identified on the dendrogram. Color coding of size classes (see online version) corresponds to that of Figure 3. Histologically sampled specimens are framed along with the corresponding symbol of their qualitative ontogenetic stage (see Fig. 3). Note that only cluster 'a' does not mix different size categories; however, size-class distribution among clusters is not random either. Agglomerative coefficient measures the clustering structure of the data set (see Maechler et al. 2013).

FIGURE 5. Composite visualization of the results of LDA testing the validity of a priori size classes. Two scatter plots of LD1-LD2 are shown to display all details on the validating classification of specimens by LDA. Color coding blue, red, black, and green (see online version) represent a priori size classes (A, B, C, and D) assigned to the specimens by us, whereas letter coding A, B, C, and D exhibits independent specimen-classification performed by LDA. Accordingly, upper right scatter plot demonstrates the number of misclassified specimens (7 in total) wherever color code of defined size class does not match letter code of LDA groups (e.g., C is green instead of black). Lower left scatter plot identifies each specimen and indicates ontogenetic stages of the eight thin-sectioned specimens by the same symbols as in Figures 3 and 4. Stacked histograms of LD1 and LD2 are shown in the lower right and upper left part of the figure, respectively.

FIGURE 6. Four specimens selected to demonstrate diversity of shapes and microanatomical features of mandibular symphyses in transverse thin sections under single plane polarizers: sp.18 (A), sp.37 (B), sp.42 (C), and sp.2 (D). Abbreviations: ds, dorsal surface; ec, erosion cavity; f, foramen; ls, lateral surface; vs, ventral surface. Scale bar, 1 mm.

FIGURE 7. Transverse and longitudinal thin sections of sp.27 showing general histological features characterizing most specimens. See online version for color references. A, Complete cross-section image with indication of some larger-scale microscopic features such as intracortical lines of arrested growth (LAGs) and secondary bone (sb) deposited in the erosion cavities (ec) under crossed plane polarizers with λ-filter. B and C, Close-ups of the section area marked by the gray square in A under crossed (B) and single plane polarizers (C) at the same magnification (10×). Longitudinally structured highly organized primary bone (l-HOPB) has a universally dark red color, whereas secondary bone is interweaving with variable optical features under cross-polarized light with λ-filter (B). Note the difference between the appearance of transversely cut osteocyte lacunae (tol) in l-HOPB and that of randomly cut lacunae (rol) in the interweaving secondary bone in both B and C. D, Complete longitudinal section image showing gross histological features like the general organization of primary bone along the long axis of the symphyses under cross-polarized light. E, F, Magnified areas indicated by the yellow and green squares in D, respectively under crossed plane polarizers. Note the optical contrast between l-HOPB and interweaving HOPB (iw-HOPB) in E, and the elongate appearance of the longitudinally cut lacunae (lol) in l-HOPB in F. Additional abbreviations: ant, anterior part of symphysis; l-rva, longitudinal to random vascular architecture; pc, primary cortex; post, posterior part of symphysis; pvc, primary vascular canal; svc, secondary vascular canal; and see Figure 6.

FIGURE 8. Transverse section of sp.18 under 10× (A) and 40× (B) magnification showing patches of woven bone (wb). Black square on A indicates the magnified area presented on B. Note the randomly oriented osteocyte lacunae in the most extensive patch of woven bone (olw)

found in this specimen and compare them with the transversely cut lacunae (tol) in l-HOPB.

For further abbreviations see Figure 7.

FIGURE 9. Scatter plot (A–C) and ordination plot (D–F) visualization of PCA and NMDS, respectively, performed on the four- (A, D), seven- (B, E), and eight-variable setup (C, F) of the histomorphometric data set. Color coding (see online version) and symbols indicate a priori size-class membership and qualitatively defined ontogenetic stages of specimens as defined in Figures 3-5. Spatial ordering of specimens reflects ontogeny with both multivariate techniques in each setup. Developmental sequence is primarily accounted for by PC1 in PCA and by axis 1 in NMDS.

FIGURE 10. Dendrograms of hierarchical cluster analysis (A, C, E) performed on the histomorphometric data set, and their corresponding LDA histograms on LD1 (B, D, F). LDA tests the strength of the two major cluster groups (a and b) identified on each dendrogram based on four (A, B), seven (C, D), and eight variables (E, F). Color and symbol codes (see online version) correspond to those in Figures 3-5.
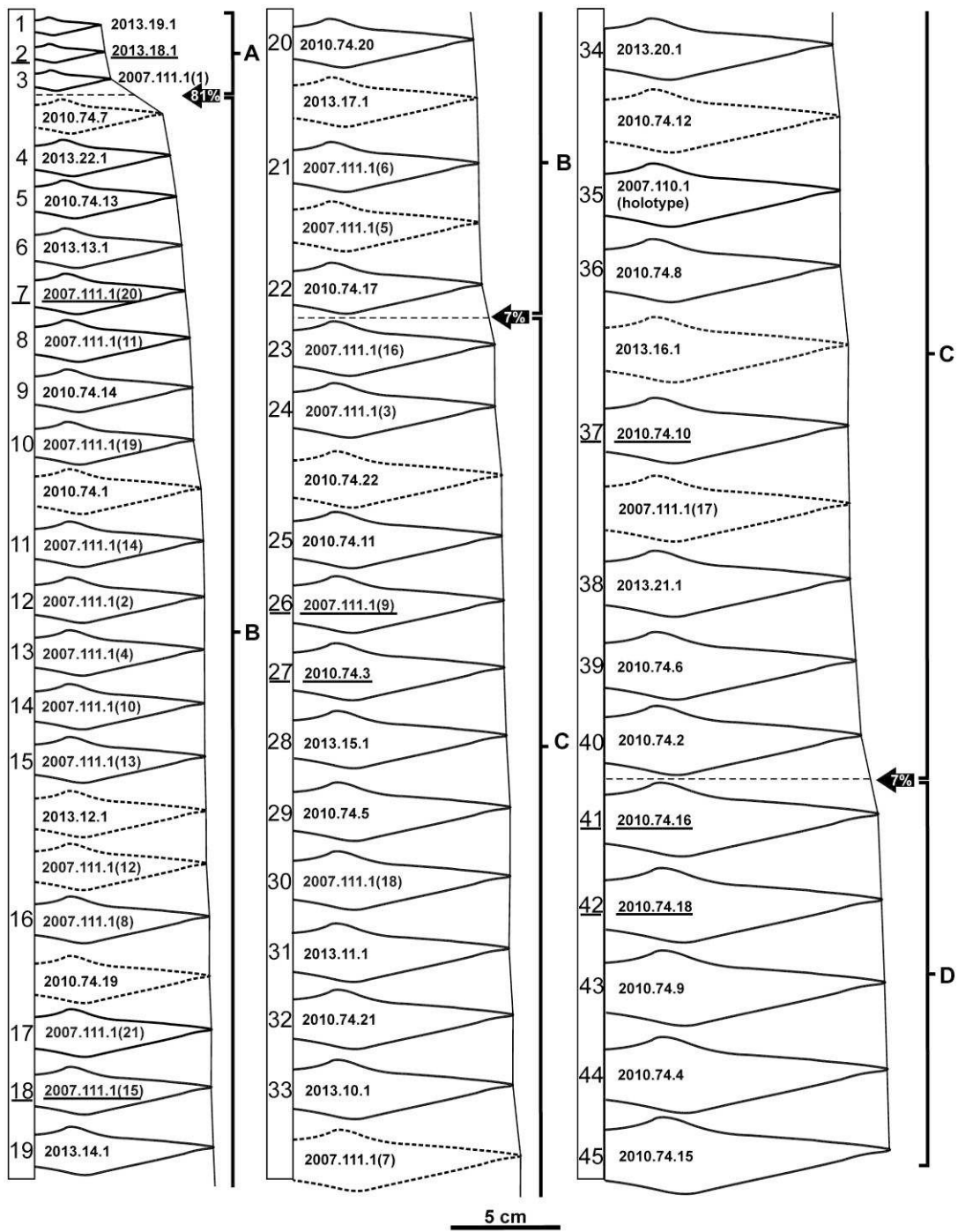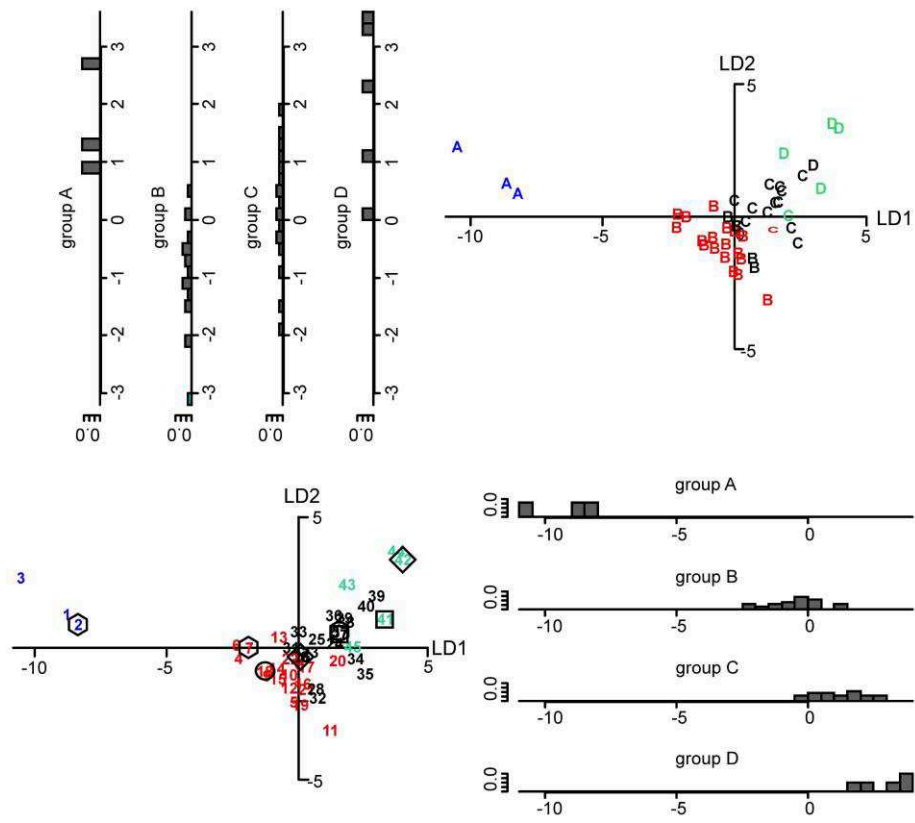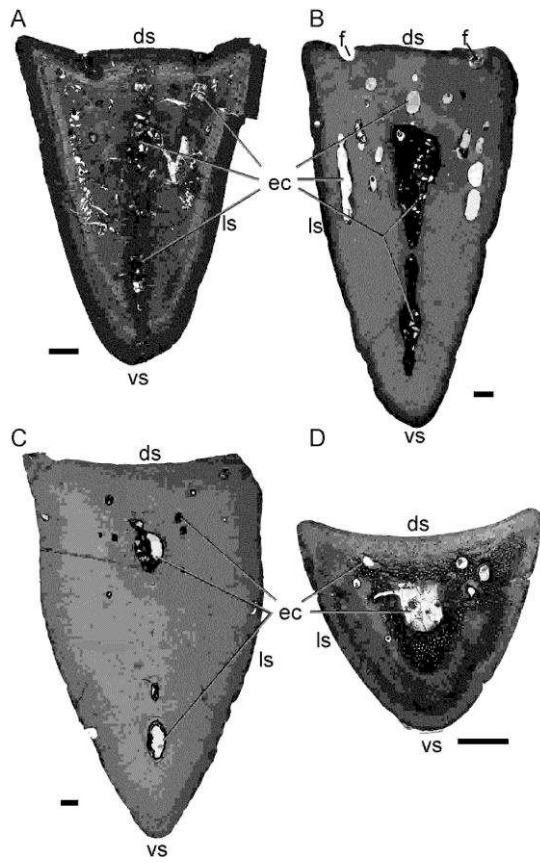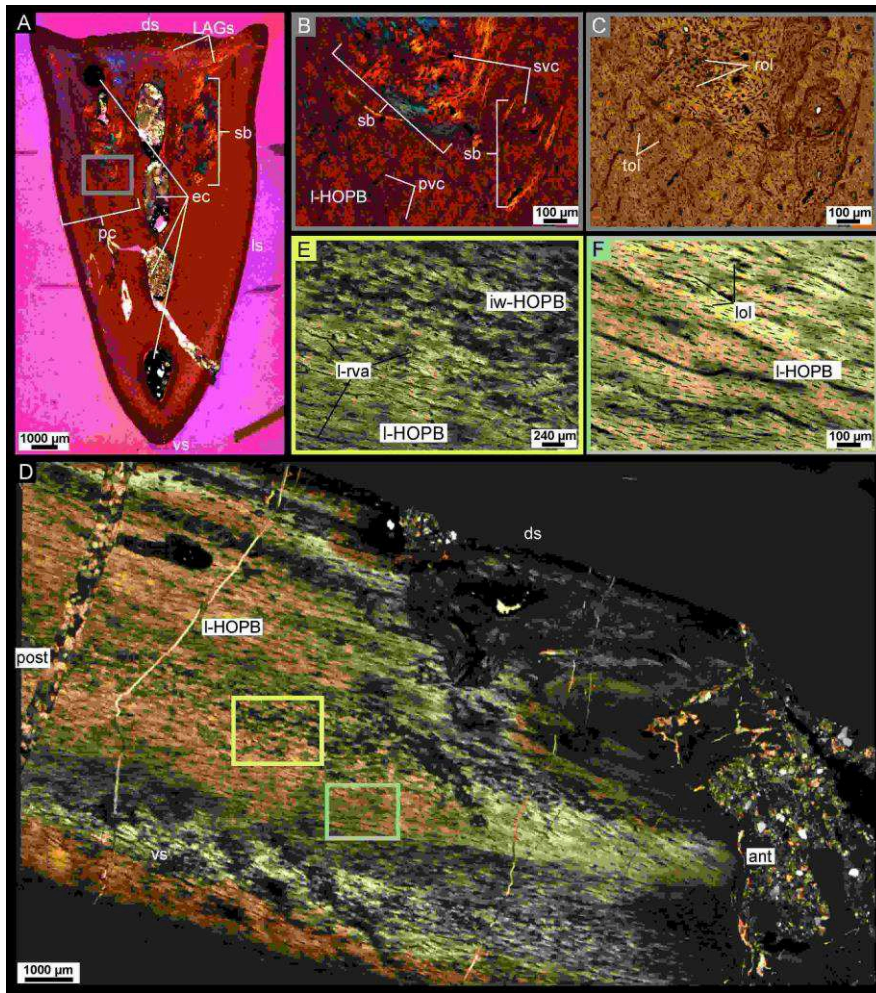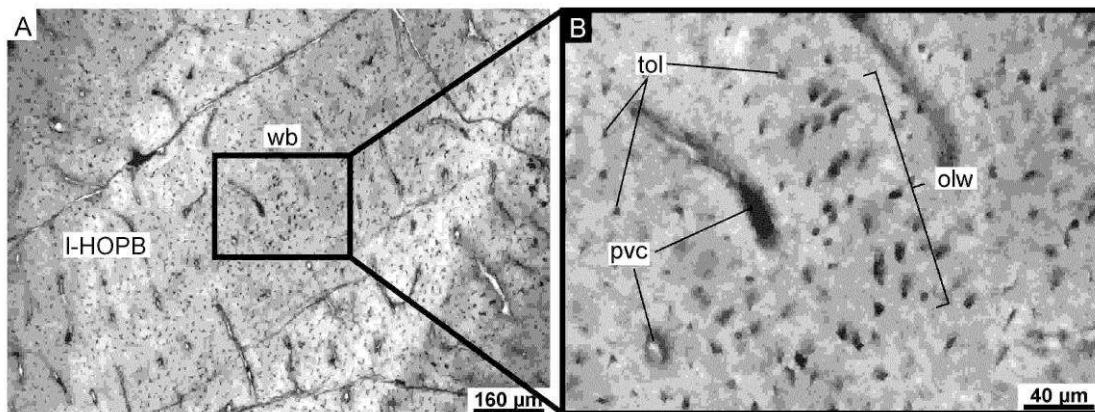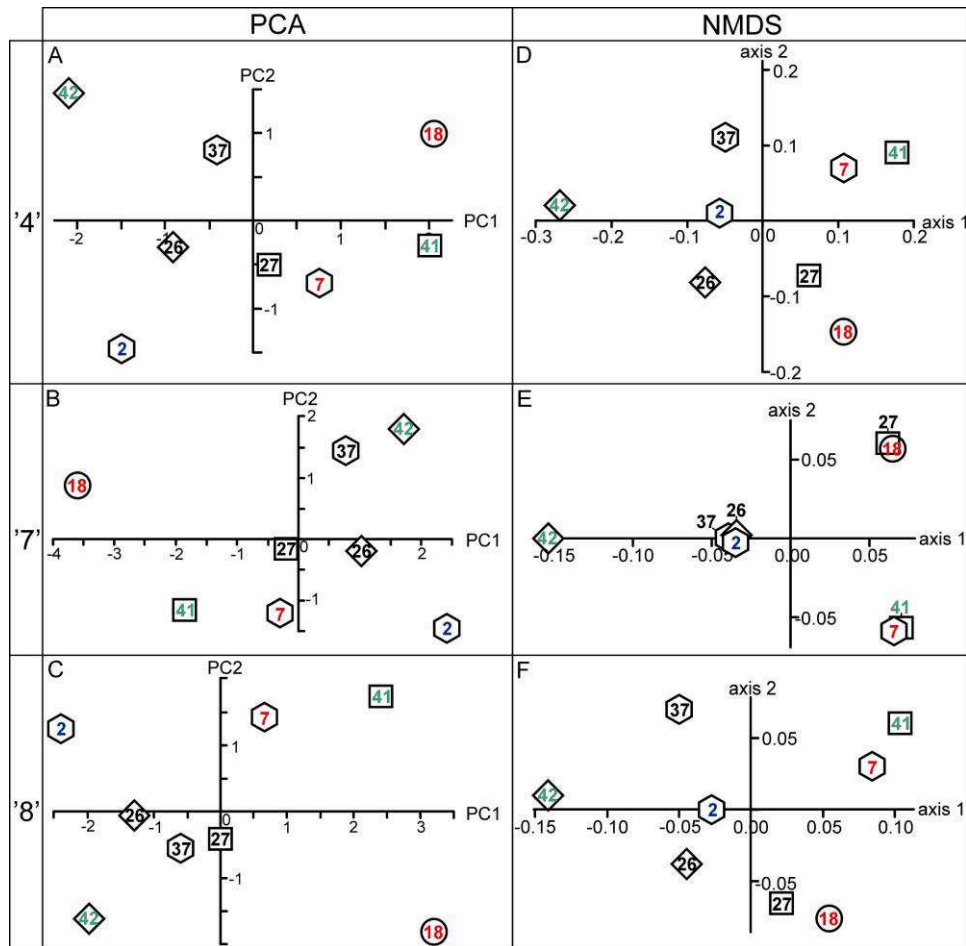
Figure 1.
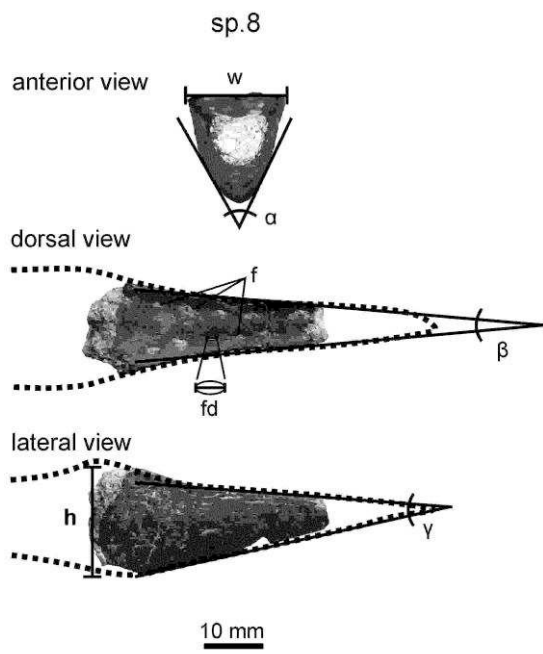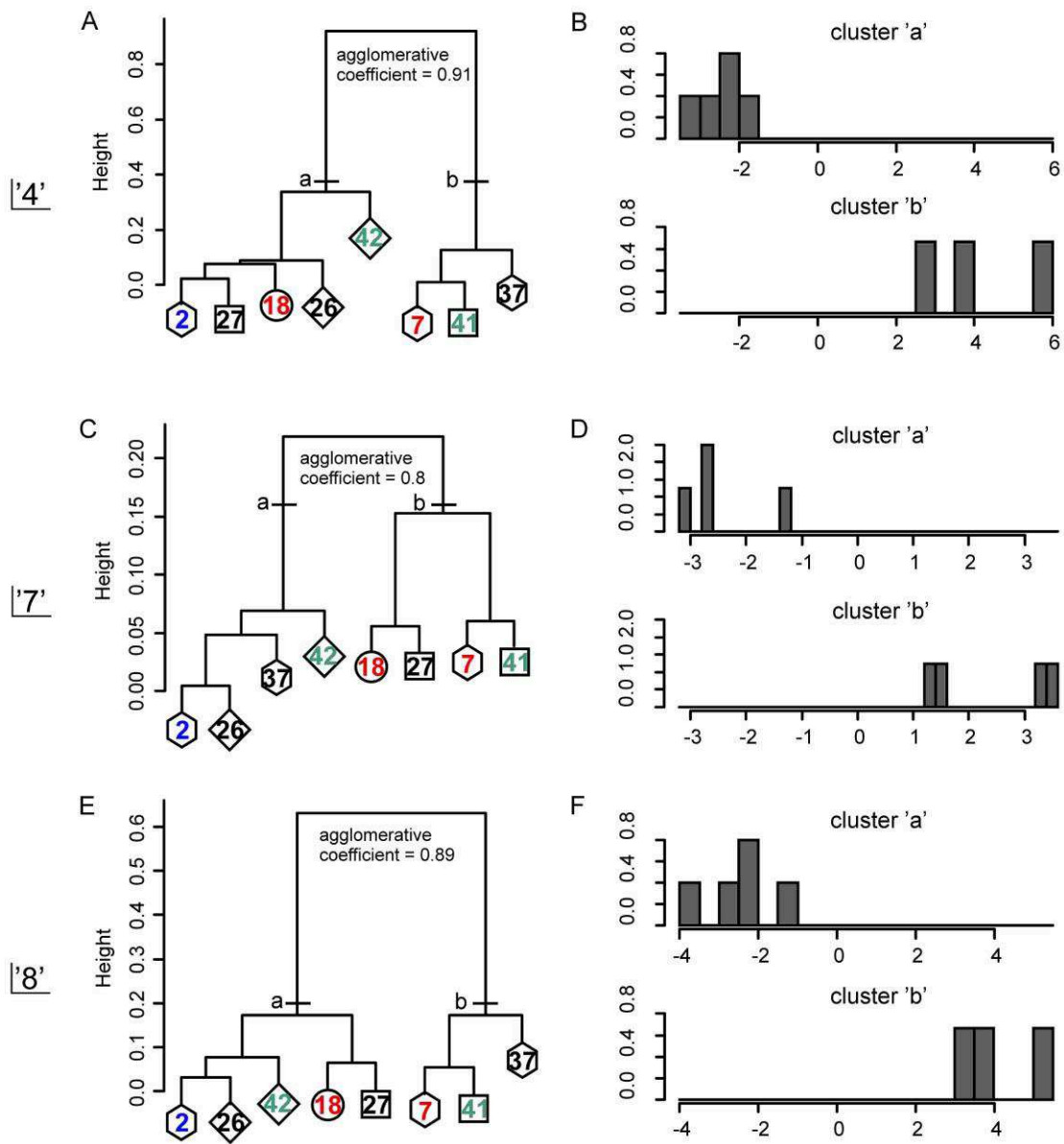
Figure 2.
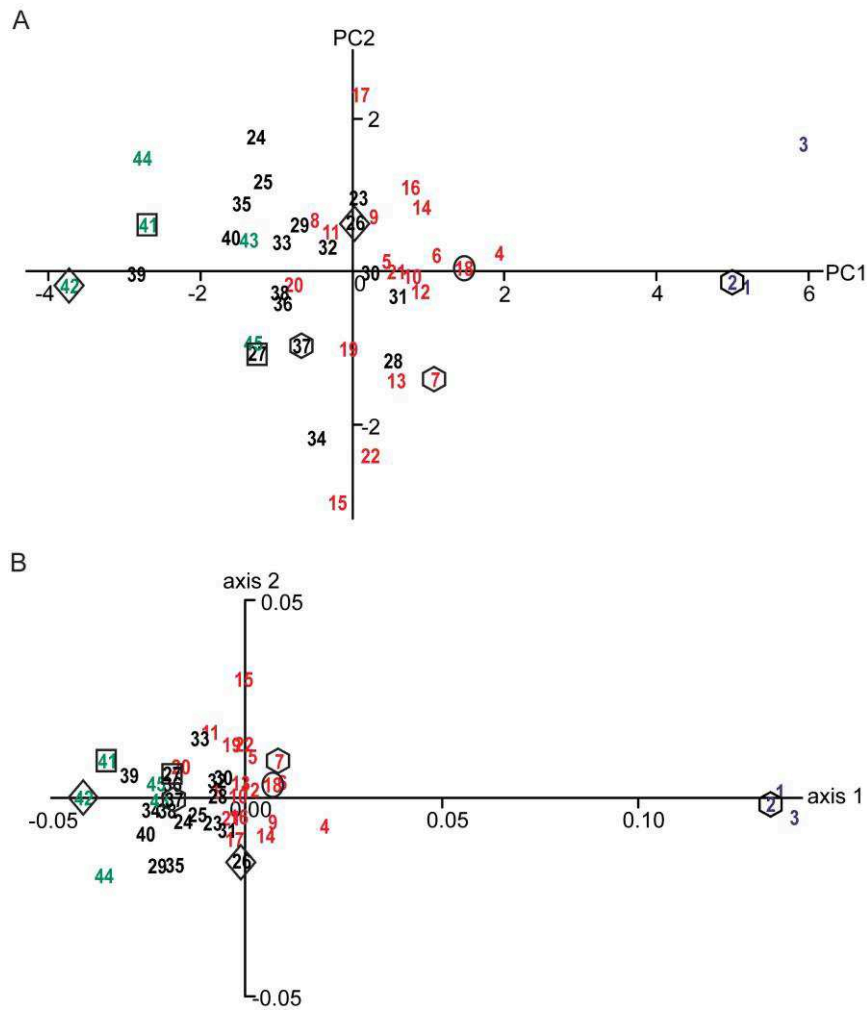
Figure 3
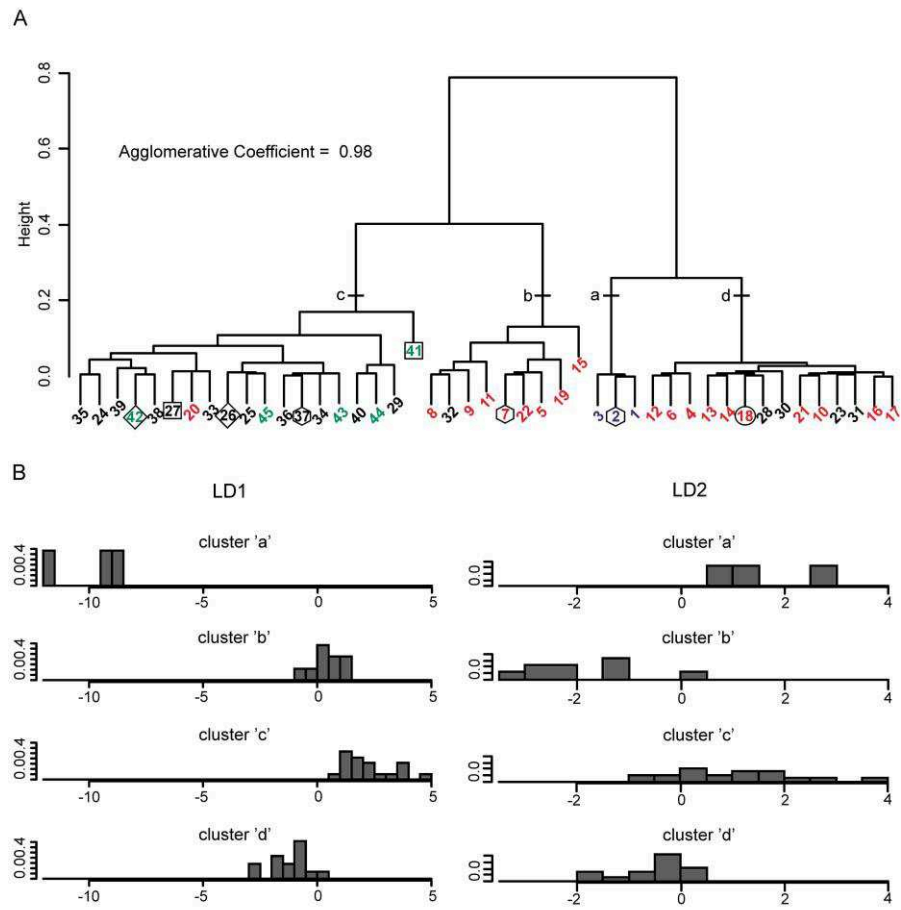
Figure 4.

Figure 5.

Figure 6.

Figure 7.

Figure 8.

Figure 9.

Figure 10.